



Originally published as:

Galbraith, C. G., Clarke, D. B., Trumbull, R. B., Wiedenbeck, M. (2009): Assessment of Tourmaline Compositions as an Indicator of Emerald Mineralization at the Tsa da Glisza Prospect, Yukon Territory, Canada. - *Economic Geology*, 104, 5, 713-731

DOI: [10.2113/gsecongeo.104.5.713](https://doi.org/10.2113/gsecongeo.104.5.713)

Assessment of Tourmaline Compositions as an Indicator of Emerald Mineralization at the Tsa da Glisza Prospect, Yukon Territory, Canada

Christopher G. Galbraith*

Department of Earth Sciences, Dalhousie University, Halifax, NS, Canada B3H 3J5

D. Barrie Clarke

Department of Earth Sciences, Dalhousie University, Halifax, NS, Canada B3H 3J5

Robert B. Trumbull

GFZ German Research Centre for Geosciences, Telegrafenberg, 14473 Potsdam, Germany

and Michael Wiedenbeck

GFZ German Research Centre for Geosciences, Telegrafenberg, 14473 Potsdam, Germany

Abstract

Tourmaline is ubiquitous at the Tsa da Glisza emerald prospect, Yukon Territory, occurring as porphyroblasts in greenschist-facies meta-volcanic and ultramafic rocks, and as crystals in granites, aplites, and quartz-tourmaline veins. The principal occurrence of emerald is along contacts between the quartz-tourmaline veins and mafic country rocks, but it also occurs in the aplites. We assess the potential of using tourmaline compositions as a guide to emerald mineralization at Tsa da Glisza based on major-element, trace-element (Li, Be, Sc, Cr, V, Mn, Ni, Co, Cu, Zn, As, Rb, Sr, Y, Zr, Nb, Cd, Mo, Sn, Sb, Cs, Ba, Ta, W, Bi, Pb, Th, and U), REE (La, Ce, Pr, Nd, Sm, Eu, Yb, Lu), and boron isotopic data. The tourmaline compositions encompass Na-Fe schorl, Na-Mg dravite, and Ca-Mg uvite and show a strong dependence on host-rock chemistry. Tourmalines closely associated with emeralds (intergrown in same hand specimen) are slightly more iron-rich dravites compared with those from schists and alteration zones lacking emerald. Binary and ternary plots of major- and trace-element concentrations show that emerald-associated tourmalines occupy restricted ranges of composition, albeit considerably overlapping those not associated with emerald. Trace-element concentrations in tourmaline associated with emerald mineralization include 20 – 40 ppm Co, ~50 ppm Ni, 0.5 ppm La, 0.5 ppm Y, 100 – 200 ppm Li, and 300 – 600 ppm Zn. Boron isotope ($\delta^{11}\text{B}$) values range from -15.6 to -4.2 ‰ for all tourmalines ($n=80$). Low values are most common, and are consistent with a dominantly granitic source of boron. Higher isotope ratios (> -8 ‰) are confined to tourmalines from country rocks and quartz veins, suggesting a contribution of isotopically heavy B from the mafic-

* Contributing author: cgeorgegalbraith@gmail.com

ultramafic series. The three emerald-related samples have a restricted, intermediate range of -10.3 to -7.9‰.

Multivariate cluster analysis defines two populations of tourmalines corresponding to host-rock type. One cluster includes tourmaline from country rocks and quartz-tourmaline veins and the other is dominated by samples from granites and aplites. The latter cluster also includes all tourmalines associated with emeralds. With trace-element concentrations and boron isotope values as input variables, one stepwise discriminant function analysis model produces a 91% correct classification matrix and an 88% correct jackknifed classification matrix. This result suggests that tourmaline has potential as an indicator mineral at the Tsa da Glisza prospect, and possibly also in the exploration for emeralds elsewhere.

Introduction

Emerald, the green variety of gem beryl, can form in a variety of environments but its occurrence invariably requires chemical input from two highly contrasting sources. Beryllium, an essential constituent of beryl, is a trace element in most rocks and tends to concentrate in felsic rocks, particularly granitic pegmatites. In contrast, the trace elements Cr and V, needed for the emerald green color, have low concentrations in felsic rocks, but high concentrations in most mafic and ultramafic rocks. One major geological setting for emerald formation worldwide is in mafic to ultramafic schists (greenstones) associated with granitic intrusions or felsic metavolcanic rocks. In these schist-hosted emerald deposits, a granitic magma or hydrothermal fluids derived from granitic or felsic volcanic bodies, provides the source for Be, Al, and Si, whereas the greenstones provide the Cr (\pm V). Examples of such schist-hosted emerald deposits are Gravelotte, South Africa (Grundmann and Morteani, 1989), Habachtal, Austria (Grundmann and Morteani, 1989; Trumbull et al., 2008b), Kafubu, Zambia (Seifert et al., 2004; Zachariás et al., 2005), Sikait-Zabara-Umm Kabo, Egypt (Grundmann and Morteani, 2007), and Khaltaro, Pakistan (Laurs et al., 1996). Tourmaline is common in association with beryl in the schist-type emerald deposits, presumably because boron concentrations also tend to be high in Be-rich plutons and their derived fluids.

This paper deals with tourmalines from the Tsa da Glisza (TdG) emerald prospect in Yukon Territory, Canada (Groat et al., 2002, 2005; Marshall et al., 2003; Neufeld, 2004; Neufeld et al., 2003,

2004; Davison, 2005), which is primarily schist-hosted and occurs within a greenstone terrane intruded by granite, aplite dikes, and hydrothermal quartz-tourmaline veins (QT). Tourmaline is widespread at TdG and occurs in the metabasic and ultrabasic schists, in granite and aplite dikes, in quartz-tourmaline veins that cut the schists, and as granular aggregates in highly-altered gossan or fault zones.

The purpose of this study is to assess the utility of tourmaline composition as an indicator mineral for emerald mineralization. Indicator minerals that are useful in exploration may be of two types. In one type, the indicator mineral or mineral assemblage is compositionally distinctive for the chemical environment of interest, and is modally much more abundant than the mineral of economic interest (e.g., chrome pyrope, chrome diopside, and magnesian ilmenite as potential indicators of diamond in kimberlite). In the other type, the indicator mineral has a wide range of chemical compositions, and can modify its chemical composition to reflect the presence of the mineral of economic interest.

Tourmaline has potential as an indicator mineral of this second type. With the formula $XY_3Z_6(BO_3)_3Si_6O_{18}(O,OH,F)_4$, the tourmaline group is one of the most chemically variable silicates, having 14 recognized mineral species (Hawthorne and Henry, 1999) and an extremely wide range of cation sizes and charges that can occupy the X, Y, and Z sites. Add to these properties the large P-T stability field of tourmaline, its propensity to develop and retain chemical zoning, and its resistance to alteration and weathering, and it thus is an excellent mineral archive. The chemical composition of tourmaline has proven useful as a proximity indicator for a range of mineral deposits (Henry and Guidotti, 1985; Jolliff et al., 1986; Clarke et al., 1989; Pirajno and Smithies, 1992; Slack, 1996; Keller et al., 1999; Yu and Jiang., 2003; Garda et al., 2003; Jiang et al., 2004). Furthermore, the B-isotope compositions of tourmaline may discriminate among different protoliths and/or fluid sources in mineral deposits (e.g., Palmer and Slack, 1989; Jiang et al., 1999; Trumbull and Chaussidon, 1999; Krienitz et al., 2008; Trumbull et al., 2008a, 2008b; Xavier et al., 2008).

The scope of our investigation of the Tsa da Glisza emerald prospect is based on in-situ microanalysis of tourmaline from 35 samples representing emerald-bearing and emerald-free assemblages in a variety of host-rock types. Our dataset comprises major- and trace-element analyses

and B-isotope ratios ($^{11}\text{B}/^{10}\text{B}$). Data interpretation is based on a combination of standard bivariate and trivariate plots, as well as multivariate statistics (cluster and discriminant function analysis).

Geological Setting

Regional geology

The Tsa da Glisza ("green stones" in the Native Kaska language; formerly Regal Ridge) emerald prospect occurs in the Pelly Mountain Range, southern Yukon Territory, several kilometers north of the Tintina Fault. This region is part of the Yukon-Tanana terrane, which is primarily composed of pre-Late Devonian metamorphosed quartz-rich meta-clastic and carbonate rocks, and Late Devonian to Mississippian metavolcanic and meta-plutonic rocks that formed in a continental arc setting (Groat et al., 2002). The principal rock types present in the vicinity of the deposit are Devonian greenschist-facies ultramafic and mafic schists and meta-plutonic rocks (Fig. 1). The ultramafic rocks consist of meta-pyroxenite and meta-peridotite, whereas the mafic rocks are boninitic metabasalt and meta-andesite that have been altered to chlorite and biotite schists, some displaying well-defined foliation. The mafic and ultramafic rocks have also undergone variable degrees of serpentinization. A Cretaceous peraluminous granitic pluton (ca. 112 Ma; Groat et al., 2002) intruded the Devonian rocks, creating a weak contact aureole and injecting an array of aplite sheets and quartz-tourmaline veins, both of which extend continuously or discontinuously for up to hundreds of meters into the greenschists. Contact metamorphism and weathering of the country rocks produced a gossan-like mass of jarosite, limonite, phlogopite, talc, and tourmaline.

Mineralization model for emerald

The quartz-tourmaline veins and aplite sheets appear to have transported beryllium and boron into the country rocks from the granitic intrusion, promoting crystallization of beryl along boundaries of the veins near the contacts with the country rock (Neufeld et al., 2003, 2004) and the widespread formation of tourmaline (Groat et al., 2002, 2005). A Cretaceous timing of mineralization is inferred from an Ar-Ar plateau age of 108.7 ± 1.2 Ma for micas associated with emerald in a schist, which supports the argument of a granite association (Groat et al., 2002, 2005). The mafic and ultramafic

greenschists are the probable sources of the chromium and vanadium (~960 ppm Cr and ~160 ppm V in bulk rock), which impart the green color to the emeralds (Groat et al., 2002), although Cr appears to be the dominant chromophore in the Tsa da Glisza emeralds (Groat et al., 2002, 2005; Neufeld et al., 2003, 2004). In addition to their elevated levels of Cr and V, the TdG emeralds also contain high concentrations of Sc and low concentrations of Fe (Groat et al., 2002). Emerald and tourmaline mineralization coincided with the later stages of regional deformation of the Devonian rocks, and with contact metamorphism from the granite (Groat et al., 2002, 2005, Neufeld et al., 2003, 2004). Geothermobarometry by Marshall et al. (2003) indicated depths of mineralization between 3 and 8 km, and temperature between 365° and 500°C. Emeralds are mainly confined to the contacts between quartz-tourmaline veins and mafic greenschists, to zones of limonite-phlogopite-talc-tourmaline alteration (Fig. 2A, B), and to mafic schist (i.e., not in the ultramafic rocks). Rarely, emeralds or colorless beryl also occur within the quartz-tourmaline veins (Fig. 2A, C) and the aplites. Field observations show that emerald-bearing rocks typically contain tourmaline, but the presence of tourmaline in veins and alteration zones does not necessarily indicate the occurrence of emeralds (see below).

Tourmaline and emeralds at Tsa da Glisza

The use of tourmaline as an indicator for emerald mineralization depends on a genetic association between these two minerals. Evidence that they are genetically related includes the following:

- (i) *Spatial* – Tourmaline and emerald occur in both the endo- and exo-contact regions of the granite body itself, and of its derivatives (aplite, pegmatite, quartz veins). Aplite and pegmatites, clearly derived from the granite, contain tourmaline and either beryl or emerald. Also, tourmaline-bearing quartz veins occur in both the granite and country rocks, and in areas where the country rocks are most affected by contact metamorphism, these veins are associated with emeralds (Groat et al. 2002; Neufeld et al. 2003, 2004).

- (ii) *Textural* – Groat et al. (2002, Figs. 8e,f) illustrated the existence of subhedral to euhedral inclusions of tourmaline in emerald, and one of our samples (Fig. 2B) shows a single quench-textured intergrowth of tourmaline and emerald in an aplite dike. Figures 2C and 2D also show intergrown tourmalines and emeralds, in some cases with their long crystallographic axes aligned in a common plane, indicating that tourmalines and emeralds are coeval at TdG.
- (iii) *Temporal* – A compilation of $^{40}\text{Ar}/^{39}\text{Ar}$ and U-Pb ages for the intrusion and mineralization at Tsa da Glisza (Mortensen et al. 1999; Groat et al. 2002) suggests that only one intrusion-mineralization event occurred in this area at 108-112 Ma.
- (iv) *Chemical* – In his chemical classification of mineralized granites, Strong (1981) identified a Be-B-Li-P group, characterized by high concentrations of these cations. By this definition, the pluton at TdG is a peraluminous Be-B-Li-P granite, and it appears to be a suitable source for both the B for tourmaline and the Be for beryl/emerald.

On the strength of this evidence that tourmaline and emerald formed in the same magmatic-hydrothermal event and are paragenetically related, we believe the conditions are met to test the potential of tourmaline composition as an indicator mineral for emerald mineralization at TdG.

Analytical Methods

Major-element analyses were obtained from polished thin sections of the 35 tourmaline-bearing rock samples. Trace-element and B-isotope analyses reported were obtained on polished grain mounts containing from 2 to 5 tourmaline grains from each sample.

Electron Microprobe

Major-element analyses of tourmaline were obtained at Dalhousie University using the JEOL 8200 electron microprobe with a spot size of 5 μm . From 5-11 points on various tourmaline grains were measured on each sample. In both the country rocks and the veins, some tourmalines display optical zoning (Fig. 2G, H). In cases of zoned tourmalines, analyses were obtained from the rims and the cores; however, only one sample (QTMO7) indicated significant chemical zoning. The mean

values are reported in Table 1a. Elements determined were: Si, Al, Na, Ca, Fe (total), Mg, Mn, Cr, V, Ti, K, and F. Jadeite was used as standard for Na, sanidine for K, Al, and Si, pyrolusite for Mn, garnet 12442 for Fe; and Kakanui kaersutite for Ca, Mg, and Ti. Pure metals were used as standards for Cr and V. Boron was not determined, and concentrations in Table 1 are reported with a constant value of 10.4 wt% B₂O₃, approximating a stoichiometric 3.00 B atoms per formula unit (apfu). The major-element concentrations, including Cr and V, were converted to apfu, based on 31 oxygens, and distributed to cation sites according to the following scheme. Elements Na, Ca, and K occupy only the X-site. If the sum Na + Ca + K is less than 1.00 apfu, the remainder represents vacancies in the X-site. The T-site is occupied by Si, and enough Al to total 6.00 cations. Elements Fe, Mn, Ti, Cr, and V occupy only the Y-site. The Mg and Al can occupy both Y- and Z-sites; whereby we assume that for Ca in the X-site, charge balance is maintained by assigning an equal amount of Mg in the Z-site (uvite component). All remaining Mg is assigned to the Y-site. Some Al can be added to the Y-site such that the sum of all cations is equal to 3.00 (i.e., $Fe + Mg^Y + Mn + Cr + V + Ti + Al^Y = 3.00$). Whatever Al remains must therefore occupy the Z-site; in all cases of TdG tourmalines, the number of cations in this site is equal to, or close to, 6.00. The F-site consists of 4.00 anions, where the assigned OH = 4.00 - F. Although O may also occupy this site, for simplicity we assume it does not. Our assessment of tourmaline as an indicator mineral is independent of the method chosen to calculate structural formulae.

Laser Ablation ICP-MS

Trace-element analyses were performed on 35 samples by Laser Ablation-Inductively Coupled Plasma-Mass Spectroscopy (LA-ICP-MS) at Memorial University of Newfoundland (MUN), using a HP4500 ICP-MS coupled to a NUWAVE UP213nm Nd:YAG laser. Elements measured were Li, Be, B, Al, Sc, Cr, V, Mn, Ni, Co, Cu, Zn, As, Rb, Sr, Y, Zr, Nb, Mo, Sn, Sb, Cs, Ba, La, Ce, Pr, Nd, Sm, Eu, Yb, Lu, Ta, W, Bi, Pb, Th, and U. Ablations were performed in helium carrier gas, which was combined with argon just prior to the feed to the torch. Nebulizer flow rates were about 0.9 l/min He and 0.75 l/min Ar. Laser energy was about 0.35 mJ (about 7 J/cm²) at a laser repetition rate of 10 Hz, producing a 80 µm diameter spot on the sample. The trace-element concentrations were calculated

using Si as an internal reference and the average SiO₂ content determined for each sample by electron microprobe analysis. Quadrupole settling time was about 2 msec and the integration (dwell) time was 10 msec on each mass. The sampling time per sweep was 0.461503 sec with an acquisition window of about 100 sec. Approximately 30 sec of gas background data (with the laser beam off) were collected prior to each 60 sec ablation of standards and unknowns. NIST glass NBS 612 was used as reference (calibration) material and analyzed in the first two and last two positions of each run; basalt glass (USGS) BCR-2G was analyzed as an unknown twice in each run. Element values for NBS 612 are from Pearce et al. (1997) and for BCR-2G are from compilations at MUN (S. E. Jackson, unpub. data). Counts-per-second data were reduced using MUN's in-house CONVERT and LAMTRACE spreadsheet programs, which employ procedures described by Longerich et al. (1996). From 5 to 7 points were analyzed on each sample with the exception of ECRFW5 that was too small for more than three points. In the zoned sample, QTMO7, analyses were obtained from various points, but there was no identifiable difference in trace elements. Furthermore, both the LA-ICPMS-MS and SIMS analyses (below) were made on embedded and polished grain fragments too thick for optical examination, so identification of "rim" and "core" domains is not unambiguous. Values in Table 2 are averages for each sample. Some individual analyses show spikes in Cs and W that probably represent mineral inclusions within the tourmaline, not noticed in optical examination but intersected by the laser.

Secondary Ion Mass Spectrometry (SIMS)

The boron isotope compositions of tourmaline were determined with the CAMECA ims6f instrument at GFZ Potsdam. The analyses were performed after ICP-MS and electron microprobe analyses on the same sample mounts after re-polishing with alumina and distilled water, ultrasonic cleaning with ethanol, and coating with a ~35nm-thick layer of high-purity gold. Only 34 of 35 samples could be measured for boron isotope concentrations; no data are reported for sample ECRFW5. The SIMS setup used a nominally 12.5 kV ¹⁶O⁻ primary beam focused to about 10 μm diameter, with a beam current of 4 nA and a count rate on ¹¹B of about 400 kHz. Prior to each analysis a three minute pre-burn was used in order to remove the gold coat and to establish equilibrium sputtering conditions. The mass-resolving power M/ΔM was 1360, which is sufficient to separate the

isobaric interference of $^{10}\text{B}^1\text{H}$ on the ^{11}B mass station and the $^9\text{Be}^1\text{H}$ peak on ^{10}B . A 50 μm -diameter contrast aperture, 1800 μm -field aperture (equivalent to a 150 μm field of view), and 50 V energy window were used with no voltage offset. Each analysis consisted of 100 scans of ^{10}B (2 s) and ^{11}B (1 s). Instrumental mass fractionation (IMF) and analytical quality were determined by replicate analyses of tourmaline reference materials dravite HS 108796, elbaite HS 98144 and schorl HS 112566 (Dyar et al., 2001) and tourmaline B4 (Tonarini et al., 2003). Internal precision for individual analyses was typically 0.3-0.5 ‰ (1 sd), and the repeatability on reference samples averaged 1 ‰ (1 sd). The variations in mass fractionation for the reference samples is less than 1.5 ‰, which we believe to be the best estimate of the reliability of the data set. Boron isotope compositions are reported in $\delta^{11}\text{B}$ notation ($\delta^{11}\text{B} = \{(^{11}\text{B}/^{10}\text{B}_{\text{sample}} / ^{11}\text{B}/^{10}\text{B}_{\text{reference}}) - 1\} \times 1000$) relative to NBS 951, which has a reported $^{11}\text{B}/^{10}\text{B}$ ratio of 4.04362 (Cantanzaro et al., 1970). Our procedure was to measure two points on each sample mount, generally one each on two separate grains, and a third point if the first two values differed by more than 2‰. This was the case for only 3 of the 34 samples, and in these, $\delta^{11}\text{B}$ variations were 4 to 6 ‰ (Table 3).

Geochemical Results

Major Elements

Tables 1A and 1B show the major-element compositions of the 35 analyzed TdG tourmalines, and their structural formulae, respectively. Figure 3A uses X-site occupancy data to determine that most of the tourmalines belong to the alkalic group of Hawthorne and Henry (1999); five samples from the country rocks and quartz-tourmaline veins are calcic in this scheme. Figure 3B shows the cation ratios $\text{Na}/(\text{Na}+\text{Ca})$ in the X-site and $\text{Fe}/(\text{Fe}+\text{Mg})$ in the Y-site, which classify most of the TdG tourmalines as intermediate dravite and schorl. Five tourmalines from mafic country rocks and quartz-tourmaline veins are compositionally different from the others and classify as uvite in this system. Major-element correlations were assessed with Pearson correlation coefficients. Element pairs with strong negative correlation coefficients ($r^2 < -0.85$) are Fe-Mg (Fig. 4A, Table 4), Ca-Na (Table 4), Ca-Al, and Mg-Al (Fig. 4B), all of which are related to cation substitution in the tourmaline structure. The only major-element pair with a strong positive correlation coefficient ($r^2 > 0.85$) is Ca-Mg, which

presumably represents the uvite substitution and a chemical influence of the mafic country rocks. As mentioned, chemical zoning is generally lacking. Significant core-rim differences occur only in sample QTMO7, where rims are Mg-rich dravite and cores are Fe-rich schorl.

Tourmaline compositions are at least partly dependent on host-rock chemistry; our results distinguish tourmalines from country rocks and granites. In general, the country rock tourmalines are uvite-dravite, whereas the granite-related tourmalines are dravite-schorl. Granite-related tourmalines are systematically higher in MnO, Al₂O₃, and Na₂O, and lower in CaO, relative to tourmalines from the country rocks (Figs. 3 – 4). Tourmaline compositions from the quartz-tourmaline veins overlap the ranges of the other two sample types. Tourmalines associated with emerald have major-element compositions that are transitional between those from country rocks and those from intrusive (Fig. 3 – 5).

Trace Elements

Table 2 presents trace-element compositions of the TdG tourmalines grouped according to host lithology, and shown as averages of up to five analyses from each of the 35 samples. A first-order feature of these data is the variability in concentrations, some of which (e.g., Zr, W, Cs) may relate to unseen mineral inclusions intersected by the laser pit. These cases show up as outliers in the dataset, and even excluding them, the standard deviation for most trace elements is over 100% of the mean for each host-rock category (Table 2). It is notable that tourmalines from emerald-bearing country rock (prefix ECR on Table 2) have lower compositional variations than tourmalines from the other country-rock samples (relative standard deviations less than 50%). This limited variation may partly reflect the smaller number of emerald-bearing vs. barren samples analyzed. Not surprising given these large variations, few trace-element pairs show strong Pearson correlation coefficients ($r^2 > 0.85$). Exceptions are positive correlations among the rare earth elements (La-Ce, La-Nd, Ce-Nd) and Y-Yb (Table 4), which are expected based on the close geochemical similarity of these elements. An exceptionally strong correlation is Li-Zn ($r^2 = 0.95$), which is not readily explained by crystal-chemical or geochemical arguments, and thus may reflect a characteristic of the local fluid-rock system. None of the element pairs shows strong negative correlations.

The mean trace-element concentrations in Table 2 show some systematic variations according to host rock type (Fig. 5). In general, tourmalines from the granitic rocks have higher concentrations of Li, Zn, Nb, Ta, REE, Pb, Th, and U than the country-rock tourmalines, and lower Sr, Sc, V, Co, and Ni. Tourmalines from quartz-tourmaline veins are not compositionally distinctive. Given the higher contents of V, Sc, Co and Ni in tourmalines from the country rocks, one might also expect higher Cr, but the ranges of Cr in granite-hosted and metabasite-hosted tourmalines are approximately the same, and both sample groups show large variations (Table 1). Tourmalines associated with emerald from TdG have similar and variably high Cr contents as those from the emerald-free samples; however, the highest Cr concentration in tourmaline in this study is 8572 ppm, from an emerald-bearing sample (ECRFW5). The trace-element data also lack any correlation of Be concentrations in tourmaline with the presence of emerald in the samples (Table 2).

Boron Isotopes

Boron isotope ratios in 80 analyses of 34 TdG tourmalines range from -17.2 to -3.8 ‰ in the $\delta^{11}\text{B}$ notation (Table 3 and Figure 6). The maximum within-sample variation is 6 ‰ and all but three samples show variations less than 2 ‰. The ranges of $\delta^{11}\text{B}$ values for tourmalines from different host rock types overlap, but the granite-hosted tourmalines, on average, are isotopically lighter than those in the country rocks. None of the tourmalines from granitic host rocks has a B-isotope composition heavier than -9 ‰, whereas about half of the country-rock tourmalines display $\delta^{11}\text{B}$ values of -8 to -4 ‰ (Fig. 6). The quartz-tourmaline vein samples have a range of B-isotope ratios that overlaps those of both other sample groups. Tourmalines from emerald-bearing samples have $\delta^{11}\text{B}$ values in the range from -11 to -6 ‰, which is intermediate and narrower than the total range at Tsa da Glisza, also a characteristic of the major- and trace-element compositions.

Previous studies have noted a general lack of correlation between chemical and B-isotope compositions in tourmaline (Krienitz et al., 2008; Trumbull et al., 2008a) and this is also true for the TdG tourmalines. Pearson correlation coefficients for $\delta^{11}\text{B}$ values and with other chemical variables are consistently low; however, $\delta^{11}\text{B}$ and Be do show a weak negative Pearson correlation coefficient

($r^2 = -0.47$) for the entire data set. This $\delta^{11}\text{B}$ - Be negative correlation increases to $r^2 = -0.71$ for tourmalines in the country rocks only (Fig. 6B).

Discussion

The significance of the chemical and boron isotopic compositions of tourmalines from TdG is two-fold: (i) the chemical variations provide evidence about the sources of elements for the tourmalines; and (ii) statistical treatment of the data shows some potential to distinguish between emerald-related and barren tourmalines.

(i) Source constraints

Groat et al. (2002) suggested that the essential element boron in the TdG tourmalines originated from the granite intrusion, as did the beryllium in the emeralds. A granitic source of boron is partly supported by our B-isotope results. A recent compilation by Marschall and Ludwig (2006) showed that tourmalines from granite and granitic pegmatite host rocks worldwide have $\delta^{11}\text{B}$ values equal to or lower than that of average continental crust at $-10 \pm 3\text{‰}$ (Kasemann et al., 2000). The relatively low B-isotope values of most TdG tourmalines (Fig. 6) are consistent with a granitic origin for the boron. However, several of the TdG tourmalines from country rocks and veins display $\delta^{11}\text{B}$ values significantly higher than -7‰ , which require a contribution of isotopically heavier boron. A likely source for heavy boron in this setting is the greenstone lithologies (Fig. 1), because MORB and, especially, seawater-altered oceanic crust have zero to positive $\delta^{11}\text{B}$ values (Palmer and Swihart, 1996). A possible analogue for the TdG data is provided by tourmaline B-isotope compositions from the Habachtal emerald deposit, which is hosted by a serpentinite-mafic schist sequence (Trumbull et al., 2008b). The range of $\delta^{11}\text{B}$ values for tourmaline in mafic schist at Habachtal is -9 to -5‰ , similar to that at TdG, whereas tourmaline from metapelite country rocks at Habachtal has considerably lower values (-14 to -10‰), typical for continental crust and in agreement with the $\delta^{11}\text{B}$ values of granite-hosted tourmalines at TdG. Trumbull et al. (2008b) interpreted the contrasting B-isotope values of Habachtal tourmaline as reflecting different fluid sources, one of regional metamorphic origin that

equilibrated with metapelites and the other of local origin confined to serpentinized shear zones in the mafic schists.

A rigorous interpretation of the isotopic composition of tourmaline from TdG requires more detailed investigations than the reconnaissance-level of this study. Nonetheless, the present findings are consistent with a two-fluid genetic model like that proposed for the Habachtal deposit. It is significant in this respect that O- and H-isotope variations in TdG emeralds reported by Groat et al. (2002) also suggest an origin involving isotopic mixing between metamorphic and magmatic fluids.

The systematic variations of major and trace-element concentrations in TdG tourmalines according to host-rock type clearly indicate contributions from both the country rocks and granitic rocks or magmatic fluid, the details of which are a complex function of element availability and solubility in the magma-fluid-rock system(s). In general, tourmalines in the mafic country rocks are dravite (Mg-Ca rich), whereas those in the granitic rocks are schorl (Fe-Na rich). Sensibly, the characteristic elements contributed by the mafic country rock source are Ca, Mg, Sc, V, Co, Ni, and Sr, and those contributed by the granite source are Na, Al, Fe, Li, Zn, Nb, Ta, REE, and Pb (Tables 1, 2). Apparently, the larger the surface area/volume ratio of the granitic component at sample sites, and/or the larger the role of fluids (QT > aplite > granite), the greater is the evidence for hybridization of granitic and country-rock components in the tourmalines.

(ii) Chemical Distinctions

Of primary interest in this study is the possible utility of tourmaline as an indicator mineral for emerald exploration. The simplest approach to compositional discrimination is the use of binary plots comparing mineralized (i.e., emerald-associated) and barren samples (Fig. 3 – 5). On such plots, tourmalines associated with emerald occupy restricted ranges of both major- and trace-element composition, which generally lie in an intermediate position relative to those of barren tourmalines from the granitic and country-rock hosts. In those simple terms, there appears to be no diagnostic composition of tourmaline that signals the presence or absence of emerald. Because Cr and V are the main chromophores distinguishing emerald from common (e.g., white to pale green) beryl, logically these elements should be high in tourmaline associated with emerald mineralization. Some TdG

tourmaline grains do have high Cr and V concentrations, and the highest Cr content in a tourmaline (8572 ppm Cr; sample ECRFW5) is a sample closely associated with emerald. However, elevated Cr concentrations (>2000 ppm) also occur in barren tourmaline samples from the country rock and granitic hosts, so Cr concentration alone is an unreliable guide for emerald mineralization. Similarly, because Be is an essential element of beryl, one might expect higher Be concentrations in tourmalines associated with emeralds, but no pattern appears to exist for Be in TdG tourmalines (Table 2, Fig. 6b), probably because of crystal-chemical limitations on Be substitution in tourmaline (Grew, 2002). A better approach may be to simultaneously examine groups of elements, such as Fe - Mn - Ni - Zn, which together outline a distinctive geochemical signature in emerald-related tourmalines.

Multivariate statistical methods are ideally suited to such an approach. They have the ability to define natural groupings (cluster analysis) among unclassified samples, or to discriminate among defined groups (discriminant function analysis), using many compositional variables simultaneously. In geological applications, such multivariate statistical procedures encounter logistical and financial disadvantages because the number of samples should ideally be large relative to the number of variables. In this respect, with our database of 34 samples and 30 variables, the statistical analysis must be considered provisional.

We performed cluster and discriminant function analyses on the TdG tourmaline data with the following restrictions and conditions:

1. Because of closure problems and tourmaline stoichiometry, the major elements Si, Al, B, Fe, Mg, Ca, and Na are not independently variable and were excluded.
2. We included the minor elements (Ti, Mn, K, Cr, V, and F) and those trace elements for which all samples have concentrations above the limit of detection, thus including Li, Be, Sc, Co, Ni, Zn, Sr, Y, Nb, Sn, Sb, Cs, Ba, La, Ce, Nd, Eu, Yb, Ta, W, Pb, Bi, U, and excluding Cu, As, Rb, Zr, Mo, Cd, Pr, Sm, Lu, and Th. The addition of $\delta^{11}\text{B}$ gives a total of 30 variables.
3. We defined two categories of tourmaline-emerald association based solely on the proximity of the two minerals, regardless of host-rock lithology. A “narrow” association (tourmaline and emerald occurring in the same hand specimen) holds for samples ECR322807, ECR322810, EAPMT1; and a “wide” association (tourmaline occurring arbitrarily within 10 m of an emerald

in outcrop) holds for the three “narrow” samples, plus samples CR322807B, CR776T4, CRFW2, APT1, QT322807A, QTFW3, QTHRT3, QTSUM1.

4. For each “narrow” and “wide” sample category, we generated two models. The "complete" model starts with and retains all 30 chemical variables, regardless of their discriminating power. The "stepwise" model starts with 30 variables, but sequentially eliminates variables which contribute least to the discrimination. A significance level of 0.15 was used as a threshold, so that at each step the variable with largest P value greater than 0.15 (smallest "F-to-remove") is dropped. The procedure terminates when no further variables can be eliminated.
5. We also produced two classification matrices for each model, one in which all the samples define the discriminant function to classify each of the samples (classification matrix), and the other in which n-1 samples define the discriminant function used to classify each nth sample (jackknifed classification matrix). Given the relatively small sample size, the jackknifed matrix is probably more meaningful.

The cluster analysis method plots all variables in multidimensional hyperspace, and then detects natural groupings (clusters) in the dataset. The investigator specifies only the number of clusters to be defined based on the context of the study and expectation that the clusters have geological meaning. In our study, we initially defined two clusters with the potential meaning being emerald-related vs. unrelated samples regardless of host lithology; or alternatively, a host-lithologic control with little or no relation to the presence of emeralds. The results of the two-cluster models (Table 5) show that the statistically-defined clusters relate mostly to host lithology. One cluster consists of tourmalines within mafic country rocks and in quartz-tourmaline veins, whereas the other cluster consists of tourmalines from granite and aplites, including the three emerald-associated tourmalines regardless of host lithology. Subsequent models run for more than two clusters did not differ significantly from the two-cluster model, and mainly resulted in isolation of outlier samples.

Discriminant function analysis (DFA) also plots all variables in multidimensional hyperspace and then finds a mathematical function of the variables that best separates the investigator-defined populations, which in our study are tourmalines with and without an emerald association (using the "narrow" and "wide" definitions of the term explained above). Table 6 summarizes all the

discriminant function solutions for the "complete" and "step-wise" modes of calculation, also explained above. Model 1 (narrow, complete) produced a 100% correct classification matrix, but the percentage of correctly-classified tourmalines in the jackknifed matrix fell to 62% (1 of 3 emerald-associated tourmalines misclassified as emerald-free, and 12 of 31 emerald-free tourmalines misclassified as emerald-associated). Model 2 (narrow, stepwise), which retained only 9 variables (Mn, Sc, V, Ni, Nb, Sn, Ba, Ce, and W), produced a 91% correct classification matrix for tourmalines associated with emerald, and the jackknifed matrix was 88% correct (with 3 of 31 emerald-free tourmalines misclassified as emerald-associated). Model 3 (wide, complete) produced a 97% correct classification matrix for tourmalines associated with emerald, but the percentages of correctly-classified tourmalines for the jackknifed matrix is only 50% (7 of 11 emerald-associated tourmalines misclassified as emerald-free, and 10 of 23 emerald-free tourmalines misclassified as emerald-associated). Finally, Model 4 (wide, stepwise), retaining only 6 variables (Co, Ni, Sr, Sn, Ba, Ce), produced an 88% correct classification matrix, and a 79% correct jackknifed matrix (2 of 11 emerald-associated tourmalines misclassified and 5 of 23 emerald-free tourmalines misclassified).

In summary, the DFA results using the "narrow" definition of tourmaline-emerald association (Models 1 and 2) produced better discriminations than the "wide" ones (Models 3 and 4). Also, based on the jackknifed results, the narrow stepwise Model 2 is preferable to the narrow complete Model 1. The "wide" models perform less well. These models tacitly assume that the chemical signal of emerald-bearing fluids influences the compositions of tourmalines growing at distances up to 10 m. The poorer performance of the "wide" model classification matrices suggests such influence does not occur. These "wide" models may still be useful from an exploration point of view, because emerald-unassociated tourmalines misclassified as emerald-associated (false positives) are preferable to the reverse case (false negatives).

In our preferred Model 2, DFA uses only Mn, Sc, V, Ni, Nb, Sn, Ba, Ce, and W as discriminators. The inclusion of V, Sc and Ni makes sense in terms of emerald mineralization, because these elements indicate input from the mafic schist, and W also makes geological sense, based on the scheelite association with tourmaline-rich zones of emerald mineralization (Groat et al. 2002; Neufeld et al., 2003). However, the absence of Cr in the DFA model is enigmatic. The B-isotope

composition of tourmalines does not contribute significantly to the discriminant function. Also, despite inclusion of $\delta^{11}\text{B}$ as a variable in the complete models, all stepwise solutions eliminated it as a variable. Finally, we note that the particular combination of elements identified as significant for discrimination in this study may be specific to the TdG deposit and thus may not be universal for schist-hosted emerald deposits generally. In any case, the outcome of this study does demonstrate the potential for DFA to distinguish between tourmalines associated with emerald mineralization and those that are not.

Conclusions

We have investigated the major-element, trace-element, and boron isotopic composition of tourmaline to evaluate its utility as an indicator mineral for emerald mineralization in the Tsa da Glisza prospect, Yukon Territory. Tourmalines occur in metamorphosed mafic-ultramafic rocks of the Devonian Fire Lake Formation as well as in granitic-aplitic veins associated with a Cretaceous granite pluton, and in quartz-tourmaline veins. The major- and trace-element data show a strong influence of host lithology on tourmaline composition. Granite- and aplite-hosted tourmalines have low boron isotope values (averages: $\delta^{11}\text{B} = -14$ to -9%), which are within the expected range for granite-sourced crustal boron. The B-isotope compositions of tourmaline from the mafic country rocks overlap with the granitic range and extend to much higher values (maximum average: $\delta^{11}\text{B} = -4\%$), which require contributions from isotopically heavy B, presumably derived from the mafic-ultramafic rocks. Quartz vein-hosted tourmalines have B-isotope compositions intermediate between those of the other two groups (averages: $\delta^{11}\text{B} = -14$ to -7%).

Simple bivariate chemical variation diagrams show that tourmalines associated with emerald have a restricted range of compositions. Any tourmaline with a composition in that restricted range may (or may not) have associated emerald. Multivariate cluster analysis distinguishes two populations of tourmaline compositions that are strongly correlated with host lithology: one associated with the country rocks and quartz-tourmaline veins, and the other with the granites and aplites. Stepwise discriminant function analysis, using only Mn, Sc, V, Ni, Nb, Sn, Ba, Ce, and W as discriminators, can successfully classify 91% of the narrowly defined populations of emerald-associated tourmaline.

We conclude that tourmaline compositions can be useful as proximity indicators for emerald mineralization. The specific DFA results for the TdG tourmalines are unlikely to be applicable to other emerald deposits because of the sensitivity of tourmaline composition to host rock composition. Nevertheless, this study demonstrates that application of multivariate statistical methods to tourmaline compositions has clear potential as a proximity indicator of emeralds and the method should be further tested and refined elsewhere.

Acknowledgements

We thank Greg Davison of True North Gems, Ltd., for the opportunity to work on this project. For expert technical assistance in the laboratories, we thank Gordon Brown and Patricia Stoffyn of Dalhousie University, Wilfredo Diegor of Memorial University, and Ilona Schäpan of GFZ Potsdam. For their constructive reviews of our manuscript, we also thank Lee Groat of the University of British Columbia and John Slack of United States Geological Survey. A Natural Sciences and Engineering Research Council Discovery Grant to D.B. Clarke covered the costs of sample preparation, microprobe analysis, and LA-ICP-MS analysis, and his opportunity to be a visiting scientist in the Chemistry and Physics of Earth Materials section of GFZ Potsdam made the international collaboration possible.

References

- Catanzaro, E.J., Champion, C.E., Garner, E.L., Maienko, G., Sappenfield, K.M., and Shields, W.R., 1970, Boric acid: Isotopic and assay standard reference materials: National Bureau of Standards Special Publication 260-17, 70 p.
- Clarke, D.B., Reardon, N.C., Chatterjee, A.K., and Gregoire, D.C., 1989, Tourmaline composition as a guide to mineral exploration: A reconnaissance study from Nova Scotia using discriminant function analysis: *Economic Geology*, v. 84, p. 1921-1935.
- Davison, J.G., 2005, 2005-2006 Activities on the Goal and RS claims, The Tsa da Glisza project, Finalyson Lake area, Yukon Territory, Canada: True North Gems Internal 43-101 Report, 67 p.

- Dyar, M.D., Wiedenbeck, M., Robertson, D., Cross, L.R., Delaney, J.S., Ferguson, K., Francis, C.A., Grew, E.S., Guidotti, C.V., Hervig, R.L., Hughes, J.M., Husler, J., Leeman, W., McGuire, A.V., Rhede, D., Rothe, H., Paul, R.L., Richards, I., and Yates, M., 2001, Reference minerals for microanalysis of light elements: *Geostandards Newsletter*, 25, p. 441-463.
- Garda, G.M., Beljavskis, P., Juliani, C., and Silva, D., 2003, Geochemistry associated with iron formation and quartz veins of the Morro da Pedra Preta Formation, Serro do Itaberaba Group (Sao Paulo, Brazil): *Anais da Academia Brasileira de Ciencias*, v. 75 (2), p. 209-234.
- Geological Survey of Canada, 2007, Pieces of a giant jigsaw puzzle: Cordilleran terranes: Natural Resources Canada, http://cgc.rncan.gc.ca/cordgeo/terrane_e.php.
- Grew, E.S., 2002, Beryllium in metamorphic environments (emphasis on aluminous compositions): *Reviews in Mineralogy and Geochemistry*, v. 50, p. 487-550.
- Groat, L.A., Hart, C.J.R., Lewis, L.L., and Neufeld, H.L.D., 2005, Emerald and aquamarine mineralization in Canada: *Geoscience Canada*, v. 32, p. 65-76.
- Groat, L.A., Marshall, D.D., Giuliani, G., Murphy, D.C., Piercey, S.J., Jambor, J.L., Mortensen, J.K., Ercit, T.S., Gault, R.A., Matthey, D.P., Schwarz, D., Maluski, H., Wise, M.A., Wengzynowski, W., and Eaton, D.W., 2002, Mineralogical and geochemical study of the Regal Ridge emerald showing, southeastern Yukon: *Canadian Mineralogist*, v. 40, p. 1313-1338.
- Grundmann, G., and Morteani, G., 1989, Emerald mineralization during regional metamorphism: The Habachtal (Austria) and Leydsdorp (Transvaal, South Africa) deposits: *Economic Geology*, v. 84, p. 1835-1849.
- Grundmann, G., and Morteani, G., 2007, Multi-stage emerald formation during Pan-African regional metamorphism: The Zababa, Sikait and Umm Kabo deposits, south eastern desert of Egypt: *Journal of African Earth Sciences*, v. 50, p. 168-187.
- Hawthorne, F.C., and Henry, D.J., 1999, Classification of the minerals of the tourmaline group: *European Journal of Mineralogy*, v. 11, p. 201-215.
- Henry, D.J., and Guidotti, C.V., 1985, Tourmaline as a petrogenetic indicator mineral: An example from the staurolite-grade metapelites of NW Maine: *American Mineralogist*, v. 70, p. 1-15.

- Jiang, S.-Y., Palmer M.R., Slack J.F., and Shaw, D.R., 1999, Boron isotope systematics of tourmaline formation in the Sullivan Pb–Zn–Ag deposit, British Columbia, Canada: *Chemical Geology*, v. 158, p. 131-144.
- Jiang, S.-Y., Yu, J.-M., and Lu, J.-J., 2004, Trace and rare-earth element geochemistry in tourmaline and cassiterite from the Yunlong tin deposit, Yunnan, China: Implication for migmatitic–hydrothermal fluid evolution and ore genesis: *Chemical Geology*, v. 209, p. 193-213.
- Jolliff, B.L., Papike, J.J., and Shearer, C.K., 1986, Tourmaline as a recorder of pegmatite evolution: Bob Ingersoll pegmatite, Black Hills, South Dakota: *American Mineralogist*, v. 71, p. 472-500.
- Kasemann, S., Erzinger, J., and Franz, G., 2000, Boron recycling in the continental crust of the central Andes from the Palaeozoic to Mesozoic, NW Argentina: *Contributions to Mineralogy and Petrology*, v. 140, p. 328-343.
- Keller, P., Robles, E.R., Pérez, A.P., and Fontan, F., 1999, Chemistry, paragenesis and significance of tourmaline in pegmatites of the southern tin belt, central Namibia: *Chemical Geology*, v. 158, p. 203-225.
- Krienitz, M.-S., Trumbull, R.B., Hellmann, A., Kolb, J., Meyer, F.M., and Wiedenbeck, M., 2008, Hydrothermal gold mineralization at the Hira Buddini gold mine, India: Constraints on fluid sources and evolution from boron isotopic compositions of tourmaline: *Mineralium Deposita*, v. 43, p. 421-434.
- Laurs, B.M., Dilles, J.H., and Snee, L.W., 1996, Emerald mineralization and metasomatism of amphibolite, Khaltaro granitic pegmatite–hydrothermal vein system, Haramosh Mountains, northern Pakistan: *Canadian Mineralogist*, v. 34, p. 1253-1286.
- Longerich, H.P., Jackson, S.E., and Gunther, D., 1996. Laser ablation inductively coupled plasma mass spectrometric transient signal data acquisition and analyte concentration calculation. *Journal of Analytical Atomic Spectrometry*, v. 11, p. 899-904.
- Marschall, H.R., and Ludwig, T., 2006, Re-examination of the boron isotopic composition of tourmaline from the Lavicky granite, Czech Republic, by secondary ion mass spectrometry: Back to normal: *Geochemical Journal*, v. 40, p. 631-638.

- Marshall, D., Groat, L.A., Giuliani, G., Murphy, D., Matthey, D., Ercit, T.S., Wise, M.A., Wengzynowski, W., and Eaton, W.D., 2003, Pressure, temperature, and fluid inclusion conditions during emerald precipitation, southeastern Yukon, Canada: Fluid inclusion and stable isotope evidence: *Chemical Geology*, v. 194, p. 287-199.
- Neufeld, H.L.D., 2004, The Tsa da Glisza emerald occurrence: Descriptive, genetic, and exploration models: Unpublished M.Sc. Thesis, University of British Columbia, 85 p.
- Neufeld, H.L.D., Groat, L.A., and Mortensen, J.K., 2003. Preliminary investigations of emerald mineralization in the Regal Ridge area, Finlayson Lake district, southeastern Yukon, *in* Edmond, D.S., and Lewis, L.L. (eds.) *Yukon Exploration and Geology 2002: Whitehorse*, Yukon, Exploration and Geological Services Division, Yukon Region, Indian and Northern Affairs Canada, p. 281-284.
- Neufeld, H.L.D., Israel, S., Groat, L.A., and Mortensen, J.K., 2004, Geology and structural setting of the Regal Ridge emerald property, Finlayson Lake district, southeastern Yukon. *in* Edmond, D.S., and Lewis, L.L. (eds.) *Yukon Exploration and Geology 2003: Whitehorse*, Yukon, Yukon Geological Survey, p. 281-288.
- Palmer, M.R. and Slack, J.F., 1989, Boron isotopic composition of tourmaline from massive sulfide deposits and tourmalinites: *Contributions to Mineralogy and Petrology*, v. 103, p. 434-451.
- Palmer, M.R., and Swihart, G.H., 1996, Boron isotope geochemistry: An overview, *in* Grew, E.S., and Anovitz, L.M., eds, *Boron: Mineralogy, petrology, and geochemistry: Reviews in Mineralogy*, v. 33, p. 709-744.
- Pearce, N.J.G., Perkins, W.T., Westgate, J.A., Gorton, M.P., Jackson, S.E., Neal, C.R., and Chenery, S.P., 1997, A compilation of new and published major and trace-element data for NIST SRM 610 and NIST SRM 612 glass reference materials. *Geostandards Newsletter*, v. 21 (1), p. 115-144.
- Pirajno, F., and Smithies, R.H., 1992, The FeO/(FeO+MgO) ratio of tourmaline: A useful indicator of spatial variations in granite-related hydrothermal mineral deposits: *Journal of Geochemical Exploration*, v. 42, p. 371-381.

- Seifert, A.V., Žáček, V., Vrána, S., Pecina, V., Zachariáš, J., and Zwaan, J.C., 2004, Emerald mineralization in the Kafubu area, Zambia: Czech Geological Survey Bulletin of Geosciences, v. 79, p. 1-40.
- Slack, J.F., 1996, Tourmaline associations with hydrothermal ore deposits. *in* Grew, E.S., and Anovitz, L.M. eds, Boron: Mineralogy, petrology and geochemistry: Reviews in Mineralogy, v. 33, p. 559-643.
- Strong, D.F., 1981. Ore deposit models – 5. A model for granophile mineral deposits. Geoscience Canada, v. 8, p. 155-161.
- Tonarini, S., Pennisi, M., Adorni-Braccesi, A., Dini, A., Ferrara, G., Gonfiantini, R., Wiedenbeck, M., and Gröning, M., 2003, Intercomparison of boron isotope and concentration measurements. Part I: Selection, preparation and homogeneity tests of the intercomparison materials. Geostandards Newsletter, v. 27, p. 21-39.
- Trumbull, R.B., and Chaussidon, M., 1999, Chemical and boron isotopic composition of magmatic and hydrothermal tourmalines from the Sinceni granite-pegmatite system in Swaziland: Chemical Geology, v. 153, p. 125-137.
- Trumbull, R.B., Krienitz, M.-S., Gottesmann, B., and Wiedenbeck, M., 2008a, Chemical and boron-isotope variations in tourmalines from an S-type granite and its source rocks: The Erongo granite and tourmalinites in the Damara Belt, Namibia: Contributions to Mineralogy and Petrology, v. 155, p. 1-18.
- Trumbull, R.B., Krienitz, M.-S., Grundmann, G., and Wiedenbeck, M., 2008b, Tourmaline geochemistry and $\delta^{11}\text{B}$ variations as a guide to fluid–rock interaction in the Habachtal emerald deposit, Tauern Window, Austria: Contributions to Mineralogy and Petrology, doi. 10.1007/s00410-008-0342-9.
- Xavier, R.P., Wiedenbeck, M., Trumbull, R.B., Dreher, A.M., Monteiro, L.V.S., Rhede, D., de Araújo, C.E.G., and Torresi, I., 2008, Tourmaline B-isotopes fingerprint marine evaporites as the source of high salinity ore fluids in iron oxide-copper-gold deposits, Carajás mineral province (Brazil): Geology, v. 36, p. 743-746.

Yu, J.-M., and Jiang, S.-Y., 2003, Chemical composition of tourmaline from the Yunlong tin deposit, Yunnan, China: Implications for ore genesis and mineral exploration: *Mineralogy and Petrology*, v. 77, p. 67-84.

Zachariáš, J., Žáček, V., Pudilová, M., and Machovič, V., 2005, Fluid inclusion and stable isotope study of quartz-tourmaline veins associated with beryl and emerald mineralization, Kafubu area, Zambia: *Chemical Geology*, v. 223, p. 136-152.

Figure Captions

Figure 1. Geological map of the Tsa da Glisza emerald prospect (modified from Neufeld, 2004), showing sample locations. Emerald-bearing samples are indicated in red text. Lithological codes: **Dum** – [Devonian] ultramafics (peridotite & pyroxenite), **Dm** – [Devonian] gabbro sills, **DFb** – [Devonian] Fire Lake mafic boninitic volcanics, **DFa** – [Devonian] Fire Lake mafic amphibolitic volcanics, **M-DKs** – [Mississippian-Devonian] Kudh Ze Kayah metasediments, **Kg** – [Cretaceous] granite, **Ka** – [Cretaceous] aplite dykes / sills, **Ed** – [Eocene] felsic porphyritic dyke.

Figure 2. Examples of emerald and tourmaline from Tsa da Glisza. **A, B**) Emeralds (green) with quartz (white), tourmaline (black), and jarosite (orange-brown) in ECR322807 and ECRSW2 hand samples. Note the quenched acicular tourmaline crystals at the far right of 2B. **C, D**) Emeralds and tourmaline in thin section: emerald crystal piercing a tourmaline crystal in ECR322807 (C), and tourmaline and emerald crystals together in ECRFW6. **E, F**) Representative tourmaline porphyroblasts in country rock: in CRHR2 the schistosity has been deformed by the tourmaline porphyroblast (E); in CR322807B the tourmaline grain overprints the schistosity and grain boundaries are less distinct than those observed in CRHR2. **G**) In sample CR322943 the country rock has been completely replaced by tourmaline. In this sample the crystals are optically zoned, but not compositionally. **H**) Sample QTMO7 was taken from a quartz-tourmaline vein, and is the only sample identifiably containing compositionally zoned tourmalines. The tourmalines began forming as schorl (green-blue cores) and ended as dravite (brown rims).

Figure 3. Major-element classification plots.

Figure 3A. Tourmaline classification on the basis of X-site occupancy (Hawthorne and Henry, 1999) shows that all samples from Tsa da Glisza plot in the Alkalic Group.

Tourmalines from intrusive rocks (granite and aplites) are the most alkali-rich, whereas tourmalines from the country rocks and quartz-tourmaline veins are more calcic. Tourmalines from emerald-bearing rocks have compositions that are transitional between those from intrusive rocks and country rocks.

Figure 3B. Tourmaline classification on the basis of Na/(Na+Ca) in the X-site and Fe/(Fe+Mg) in the Y-site shows the influence of host rock on tourmaline compositions. Tourmalines from the granite-aplite intrusive rocks contain the highest concentrations of Na and Fe (dravite-schorl). The tourmalines from the country rock contain lower concentrations of Fe and Na (dravite-uvite). Tourmalines from quartz-tourmaline veins generally have compositions similar to those in the country rocks. Emerald-associated tourmalines, independent of host rock lithology, have intermediate Na-Fe concentrations.

Figure 4. Major-element variation diagrams.

Figure 4A. Contents of Fe and Mg in the Y-site for Tsa da Glisza tourmalines. The more magnesian tourmalines from intrusive rocks overlap with those from the country rocks, tourmalines from the Q-T veins are mainly like those of the country rocks, and the tourmalines from emerald-bearing rocks lie near the region of overlap.

Figure 4b. Z-site contents of Al and Mg in Tsa da Glisza tourmalines. Tourmalines from country rocks have the highest Mg Z-site occupancy, corresponding to charge balance by Ca²⁺ in the X-site. Tourmalines from intrusive rocks have the highest Al (Z) contents. Tourmalines from emerald-bearing country rocks are intermediate in composition.

Figure 5. Trace-element variation diagrams.

Figure 5A. Variation of Be and Cr in Tsa da Glisza tourmalines. Tourmalines show generally narrow ranges in concentration of Be (15-55 ppm) and wide ranges in concentration of Cr (0-2500 ppm). In general, tourmalines from country rocks contain the greatest variation in both elements. Tourmalines associated with emeralds show a highly restricted range of Be (~35 ppm), but a wide range of Cr concentrations. One sample from an emerald-bearing rock (ECRFW5) contained anomalously high concentrations of both Be and Cr, which may be indicative of an unseen emerald inclusion.

Figure 5B. Variation of Co and Ni in Tsa da Glisza tourmalines. Concentrations of Ni and Co in tourmalines from Tsa da Glisza are strongly correlated, but the fields of different

tourmaline groups overlap. Tourmalines from emerald-bearing schists contain restricted ranges of Co (15 - 35 ppm) and Ni (50 – 100 ppm). The tourmaline from the emerald-bearing aplite is a compositional outlier compared with the other emerald-associated tourmalines and with respect to other tourmalines from the granite/aplite-association.

Figure 5C. Variations of Yb and Y in Tsa da Glisza tourmalines shows a narrow range in concentrations, and the expected strong linear relationship. Tourmalines from emerald-bearing samples contain low concentrations of Y and Yb, compared to most others from Tsa da Glisza.

Figure 5D. Variations of Li and Zn in Tsa da Glisza tourmalines show a strong positive correlation. Tourmalines from the intrusive rocks show a different trend from that defined by most tourmalines hosted by country rocks and Q-T veins, although the two trends overlap at low concentrations. Tourmalines from emerald-bearing rocks occupy a position more closely related to the intrusive-rock trend.

Figure 5E. Variation of La and Ce in Tsa da Glisza tourmalines, showing a strong positive correlation and dependence on host lithology (no overlap between country rocks and intrusives). Tourmalines from emerald-bearing rocks contain a restricted range of both La (0.3 – 0.7 ppm) and Ce (0.3 – 1.7 ppm) and fall entirely within the country-rock field.

Figure 6. Boron isotope variation diagrams.

Figure 6A. Histograms of $\delta^{11}\text{B}$ distribution in tourmalines from the three Tsa da Glisza host lithologies. The left column of histograms presents all measured values, including duplicate and triplicate analyses on the same grains (Table 3). The right column of histograms presents the sample means for the country rock (CR), Q-T veins, and intrusive rocks. The intrusive-hosted tourmalines show a narrower range of $\delta^{11}\text{B}$ values than the other two groups, and no values heavier than -9‰. The isotopic ranges for country rock and Q-T vein tourmalines are indistinguishable.

Figure 6B. Variation of Be contents vs. $\delta^{11}\text{B}$ values in Tsa da Glisza tourmalines. Overall, the two variables show a weak negative correlation, but in detail, this correlation holds only for

the country rock-hosted tourmalines. Note the restricted range of compositions of the emerald-associated tourmaline within the country-rock field. Tourmalines associated with emerald do not have high concentrations of Be.

List of Tables (full captions are on the tables)

Table 1A. Average major-element compositions of Tsa da Glisza tourmalines (wt %).

Table 1B. Structural formulas of Tsa da Glisza tourmalines (atoms per formula unit - apfu).

Table 2. Average trace-element compositions of Tsa da Glisza tourmalines (ppm).

Table 3. Boron isotope compositions of Tsa da Glisza tourmalines ($\delta^{11}\text{B}$).

Table 4. Notable Pearson and Spearman correlation coefficients for Tsa da Glisza tourmalines.

Table 5. Summary of cluster analysis for Tsa da Glisza tourmalines.

Table 6. Summary of discriminant function analysis.

Figure

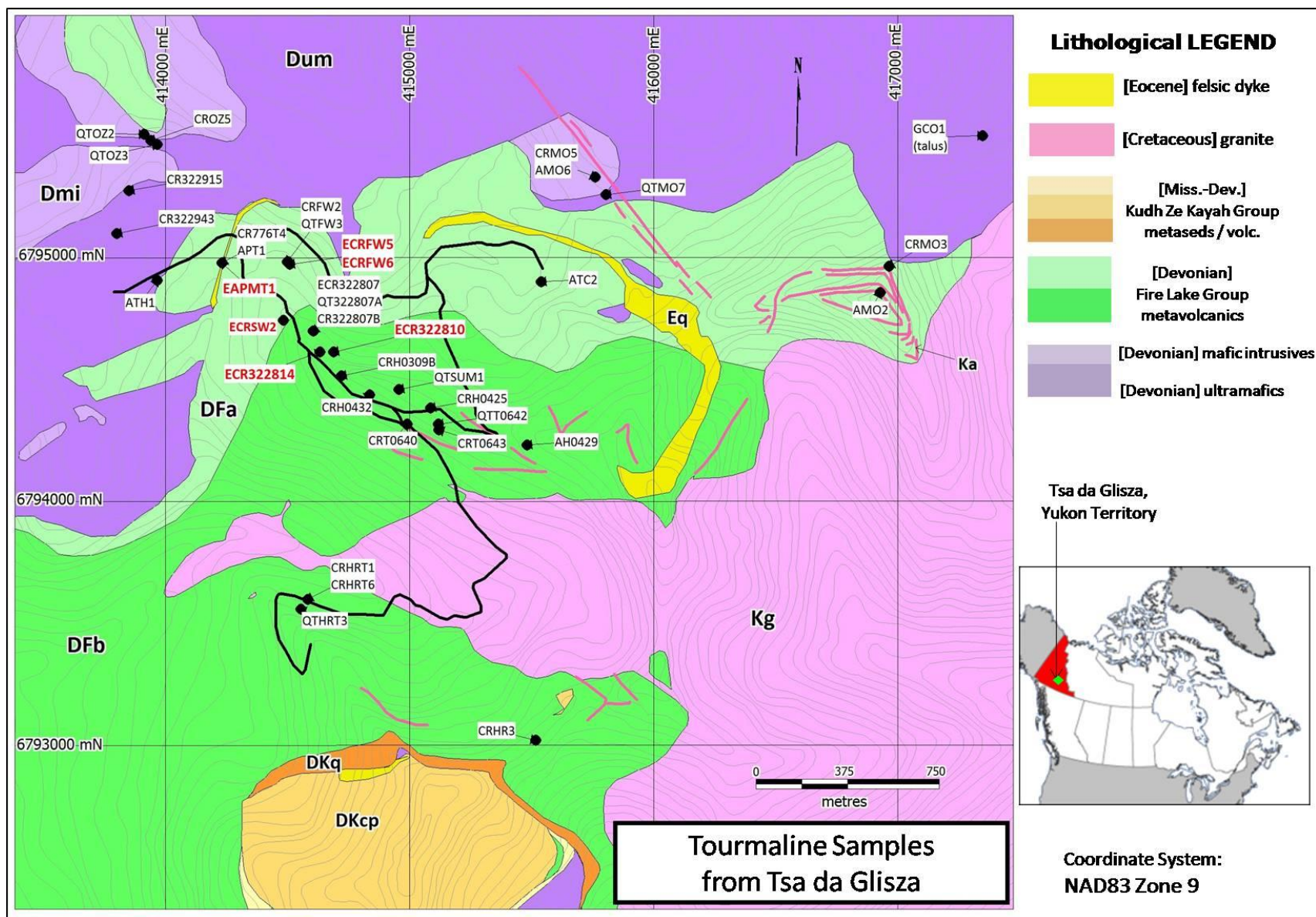


Figure 1.

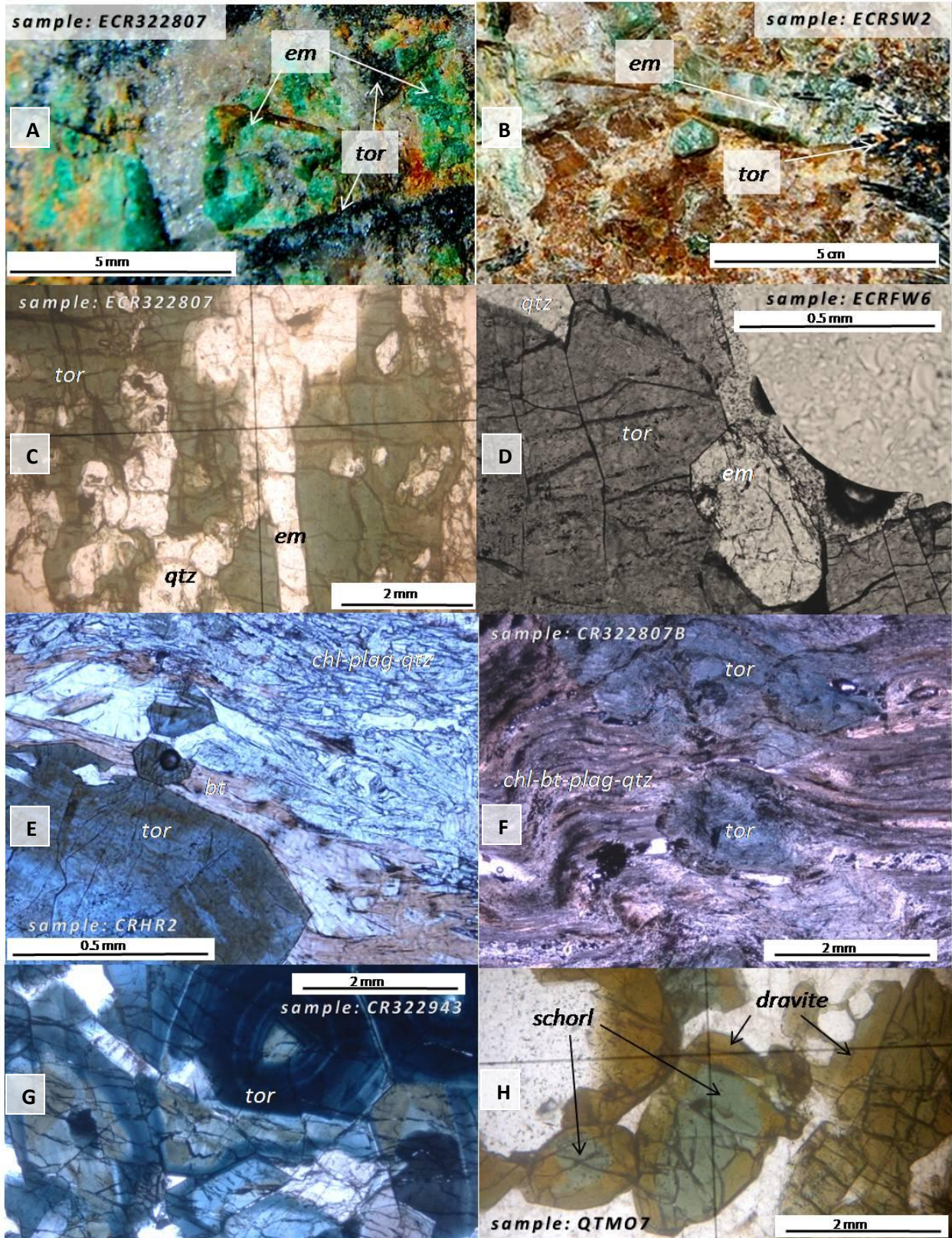


Figure 2.

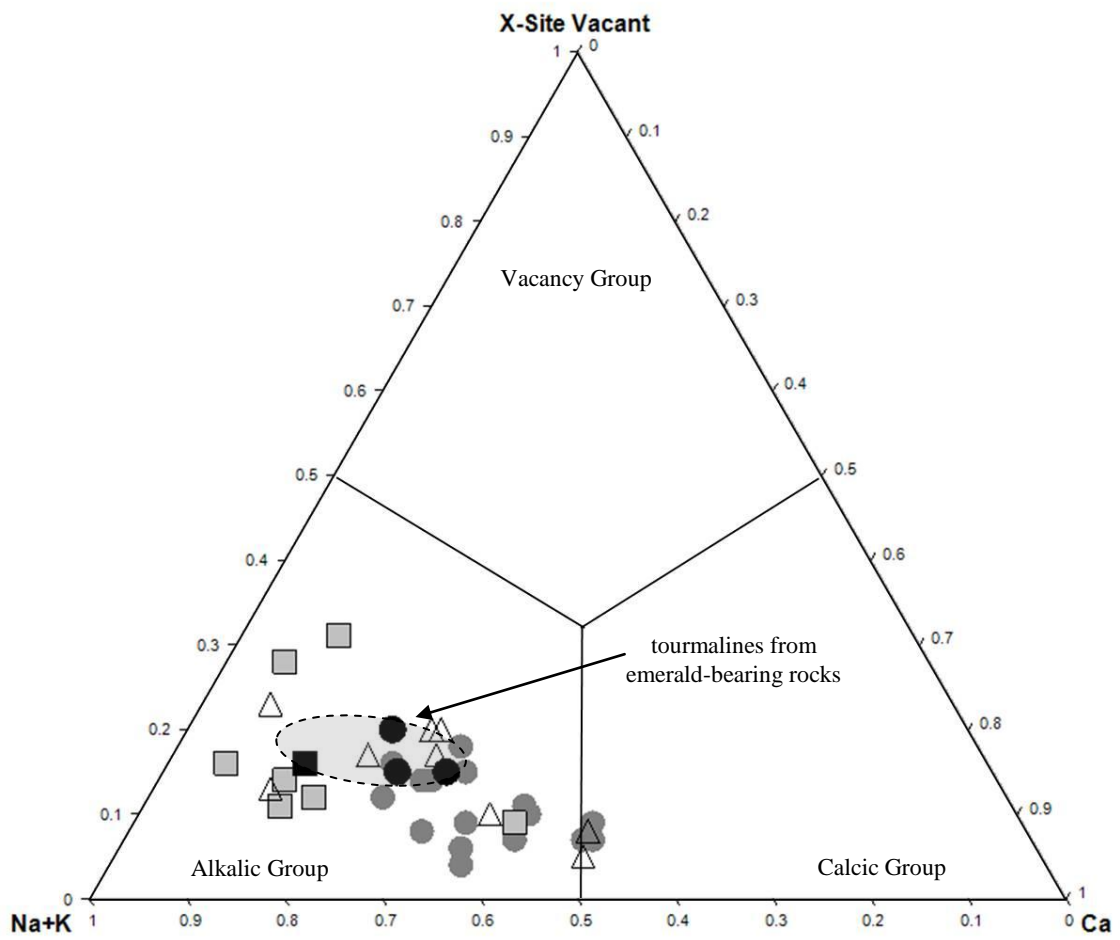


Figure 3A.

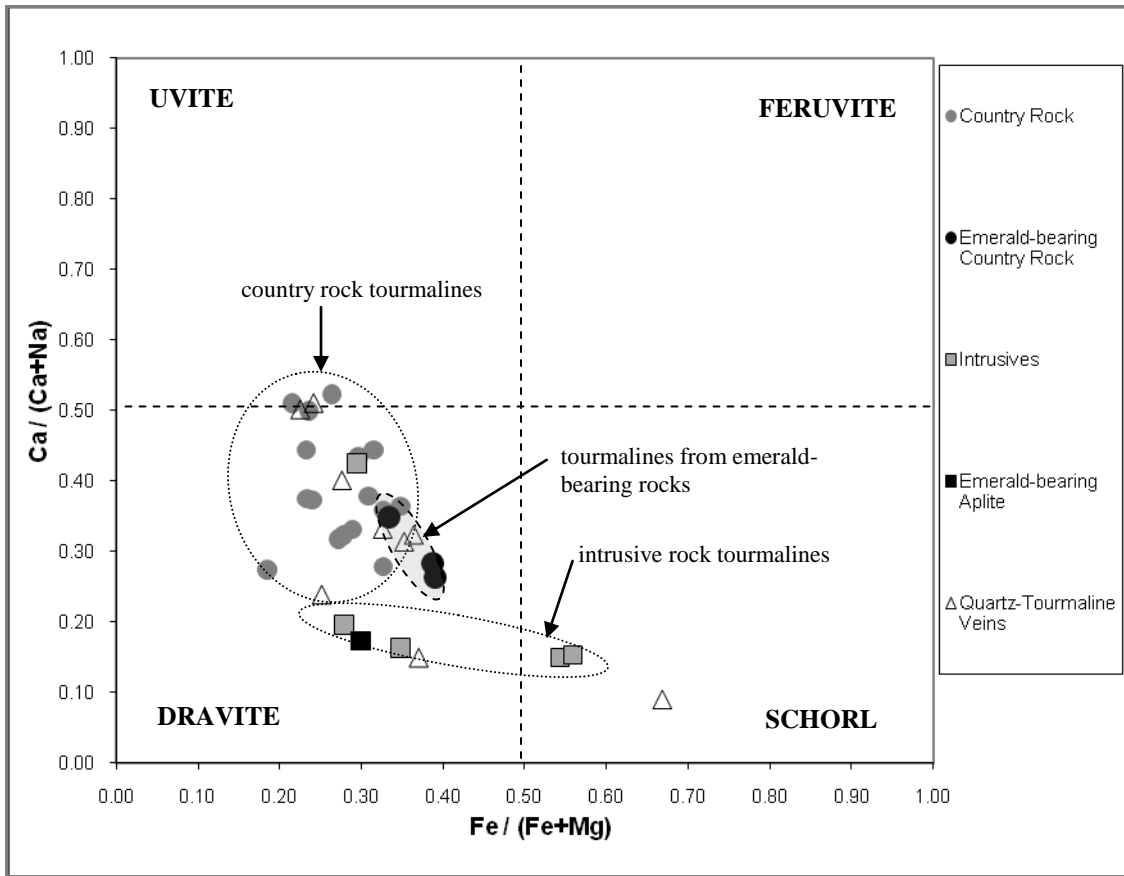


Figure 3B.

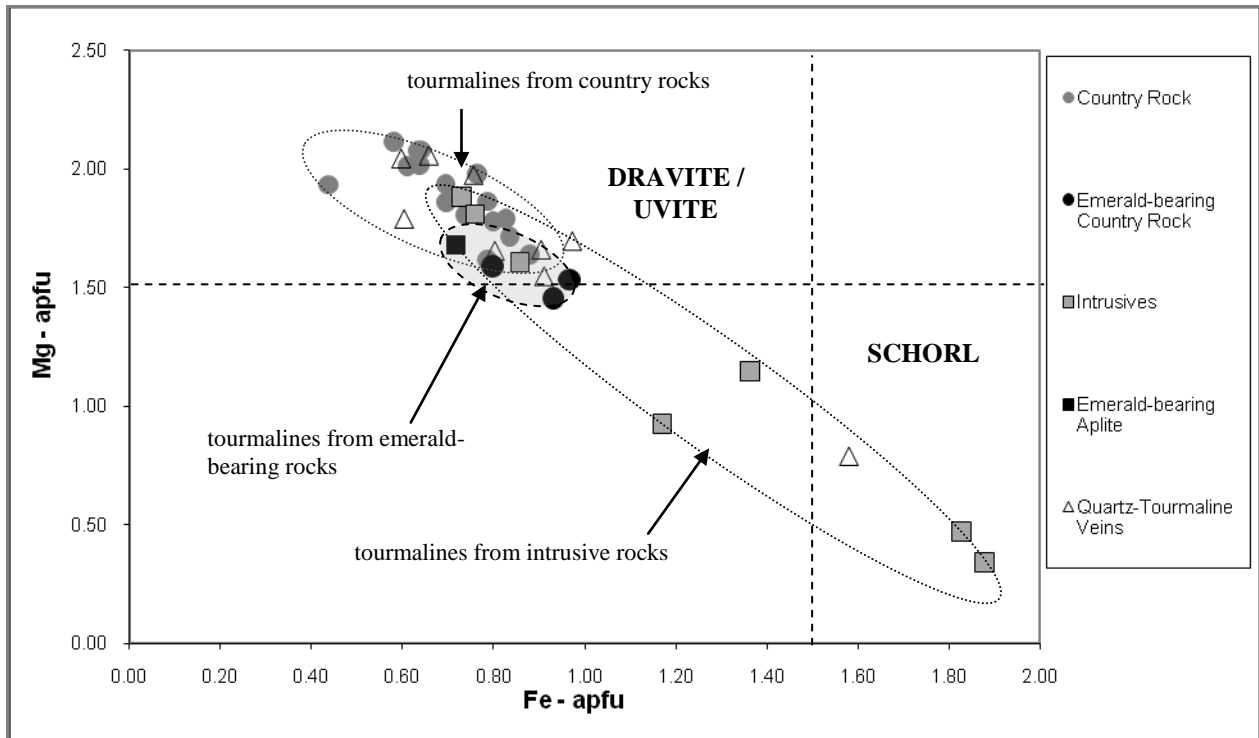


Figure 4A.

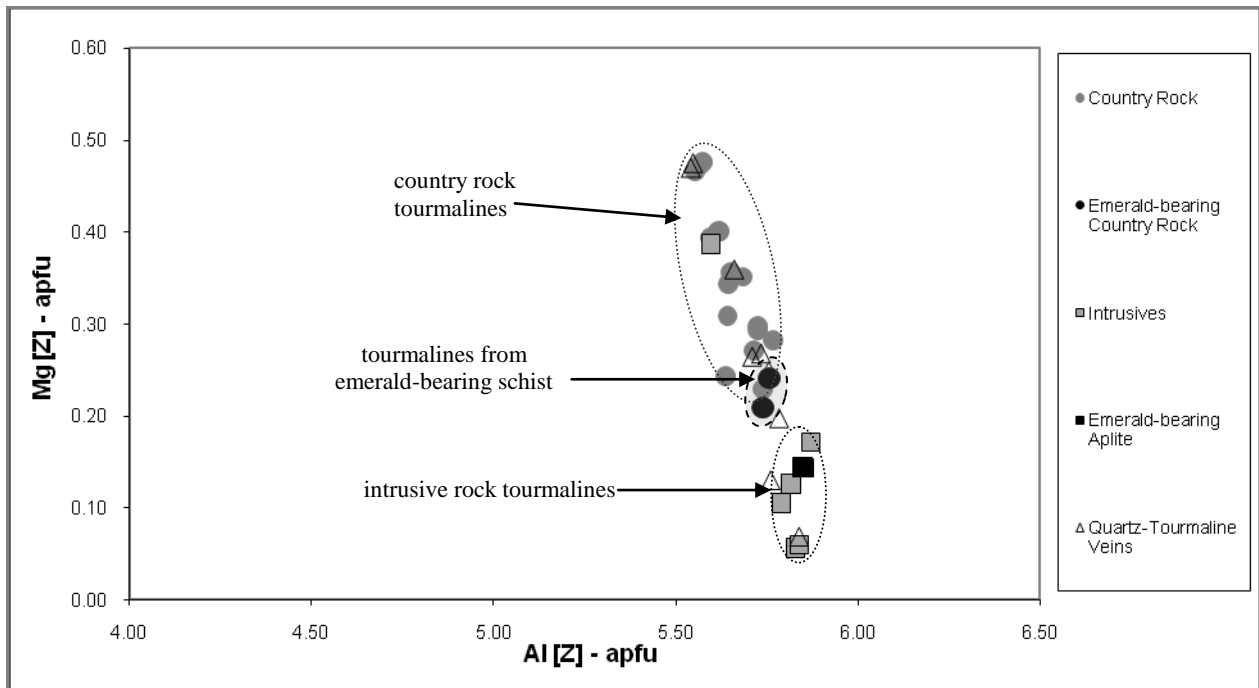


Figure 4B.

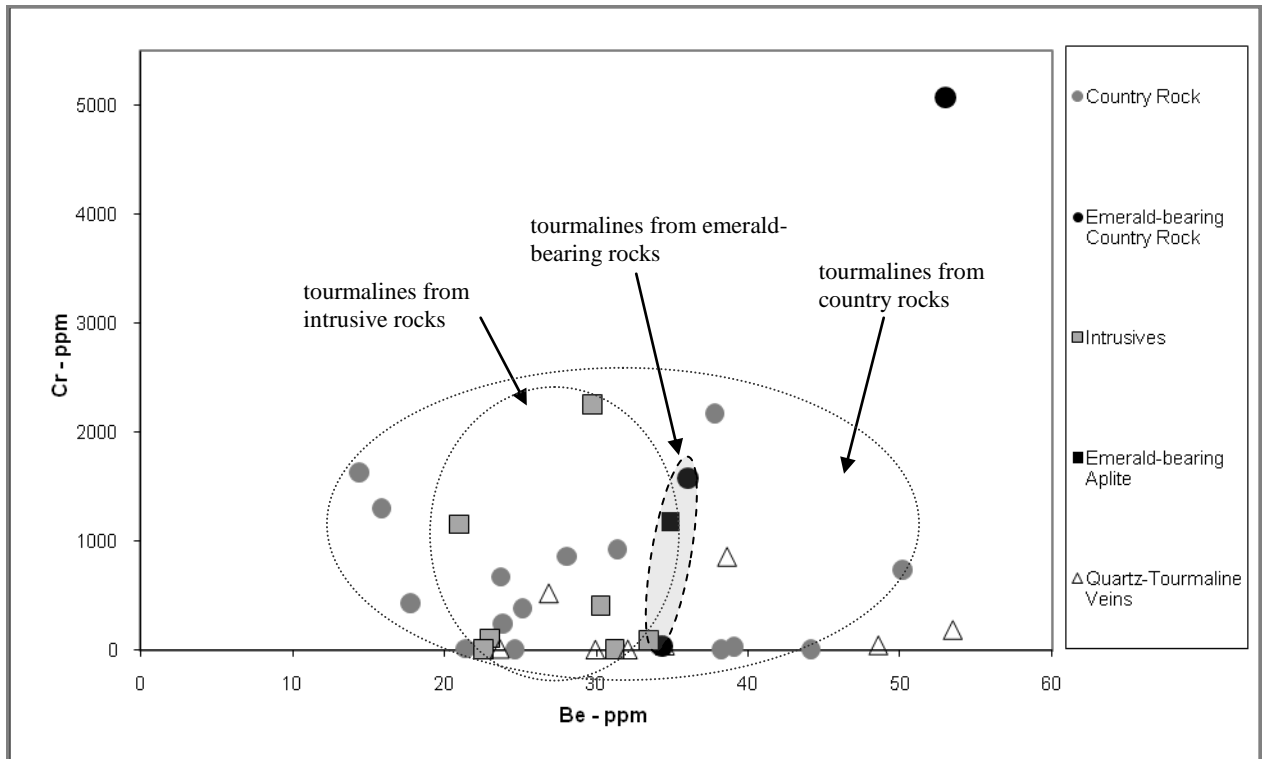


Figure 5A.

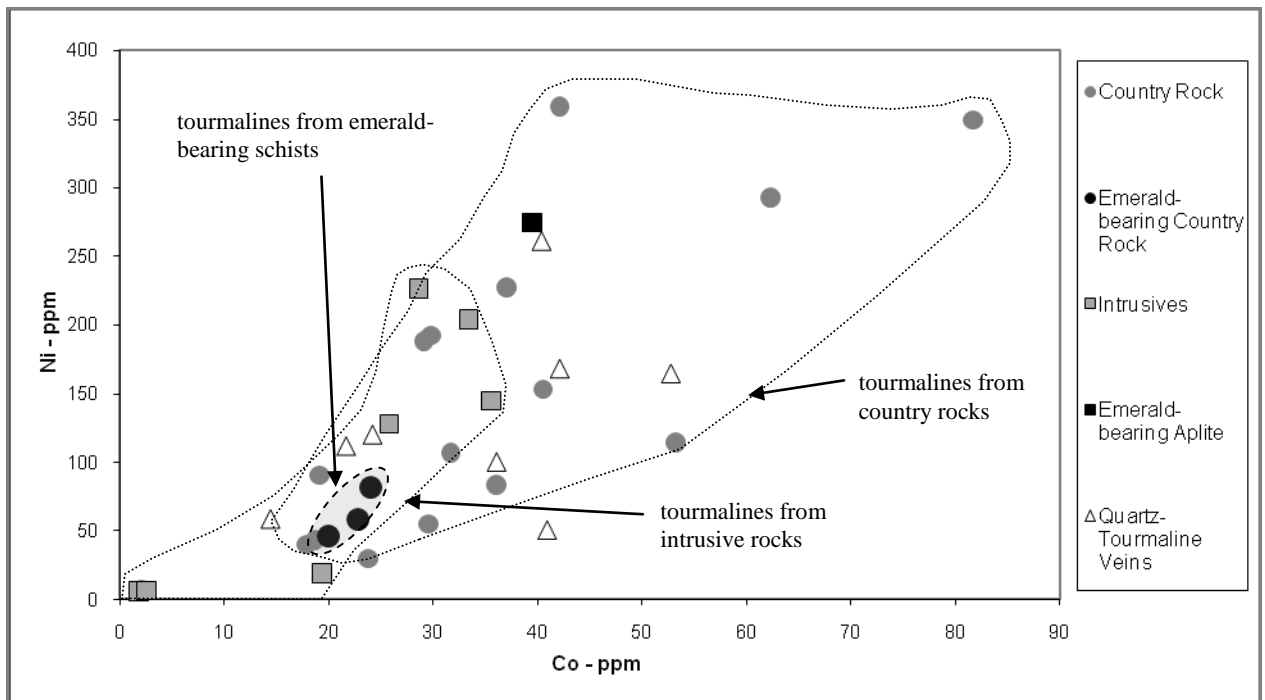


Figure 5B.

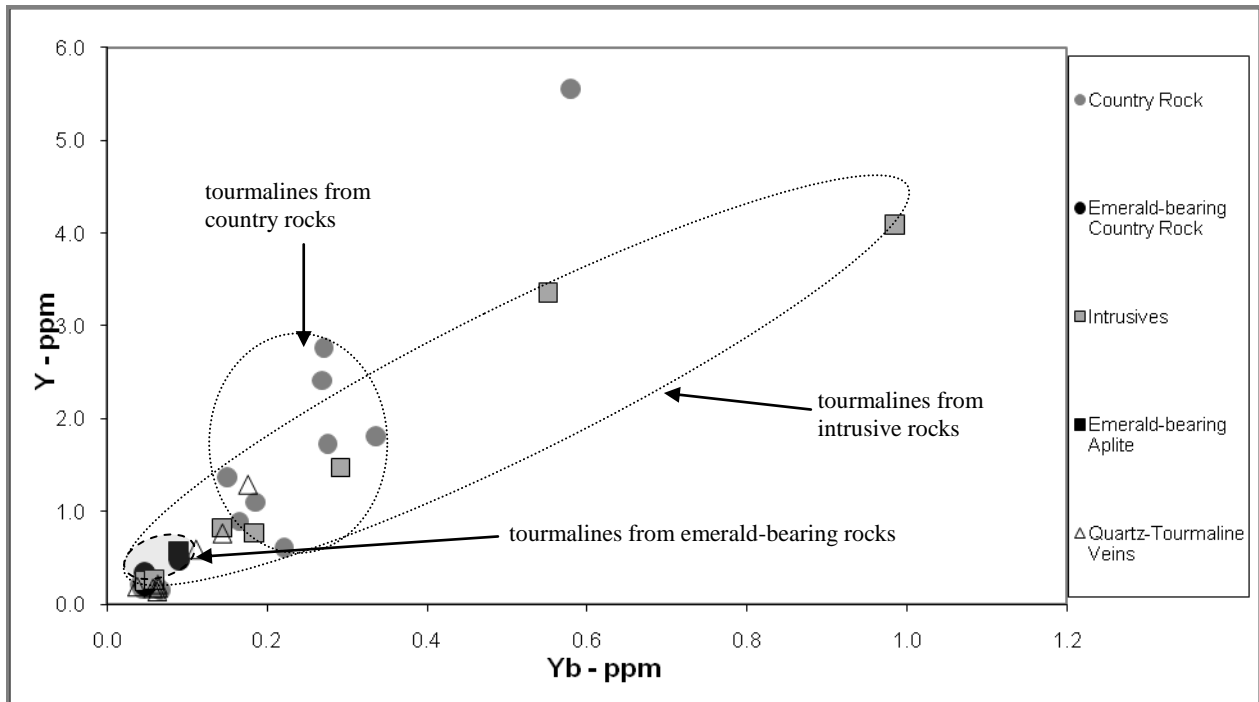


Figure 5C.

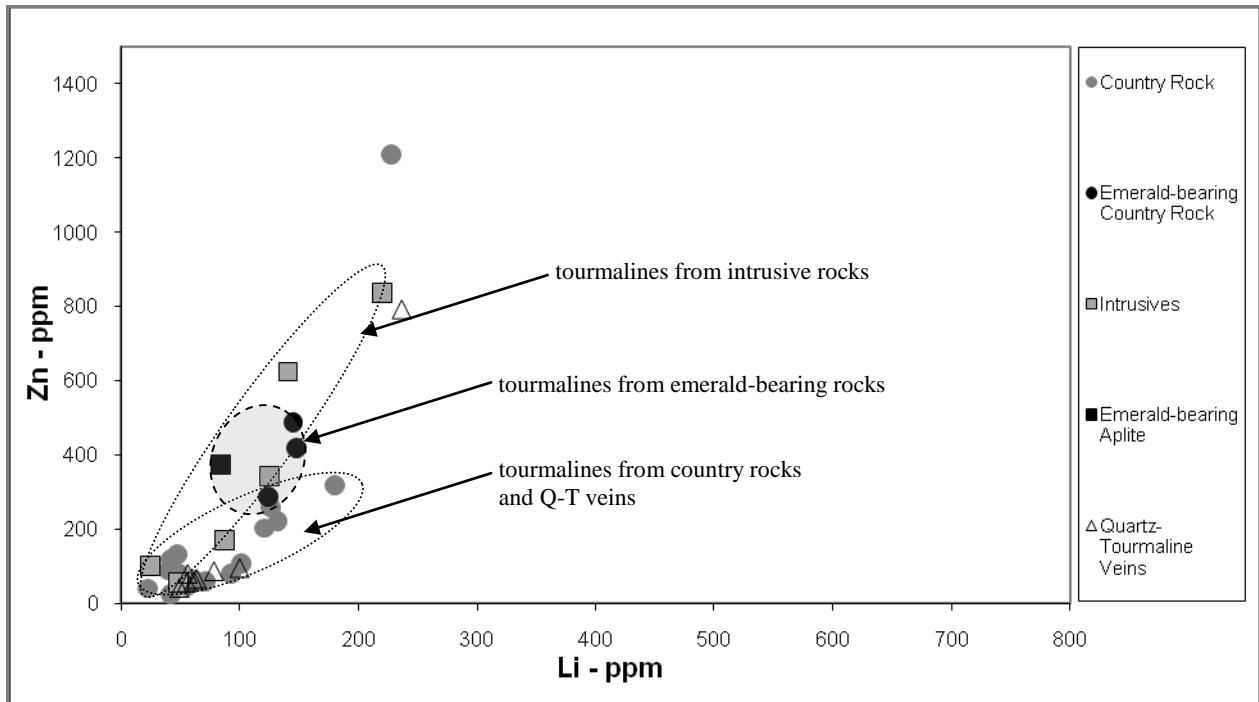


Figure 5D.

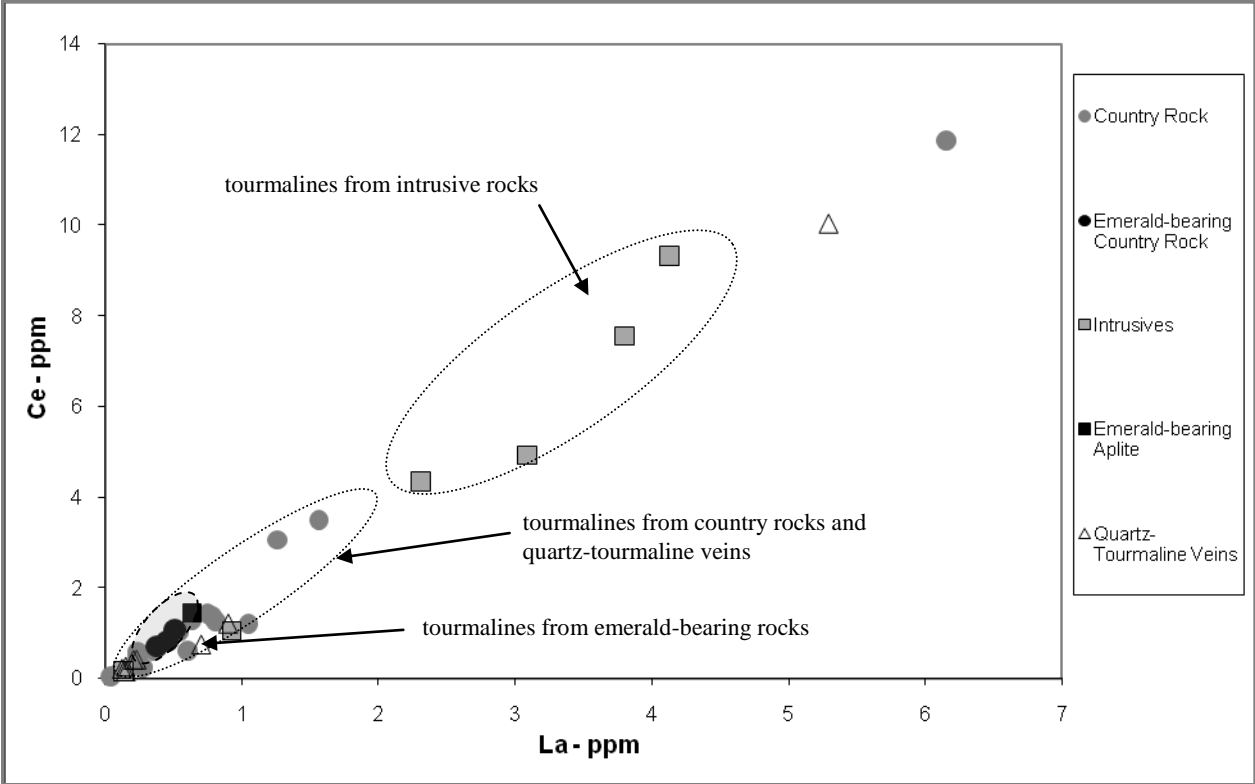


Figure 5E.

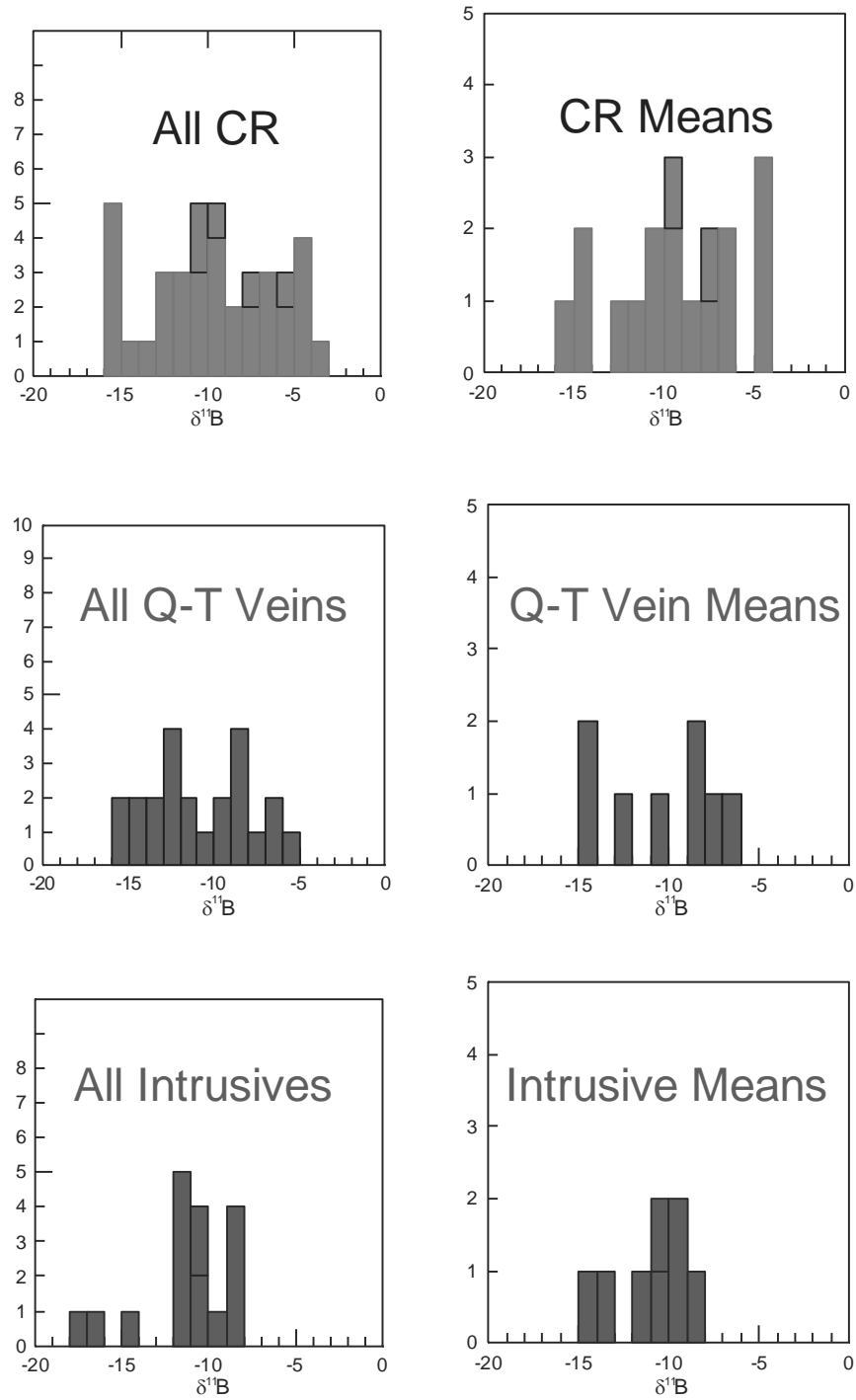


Figure 6A.

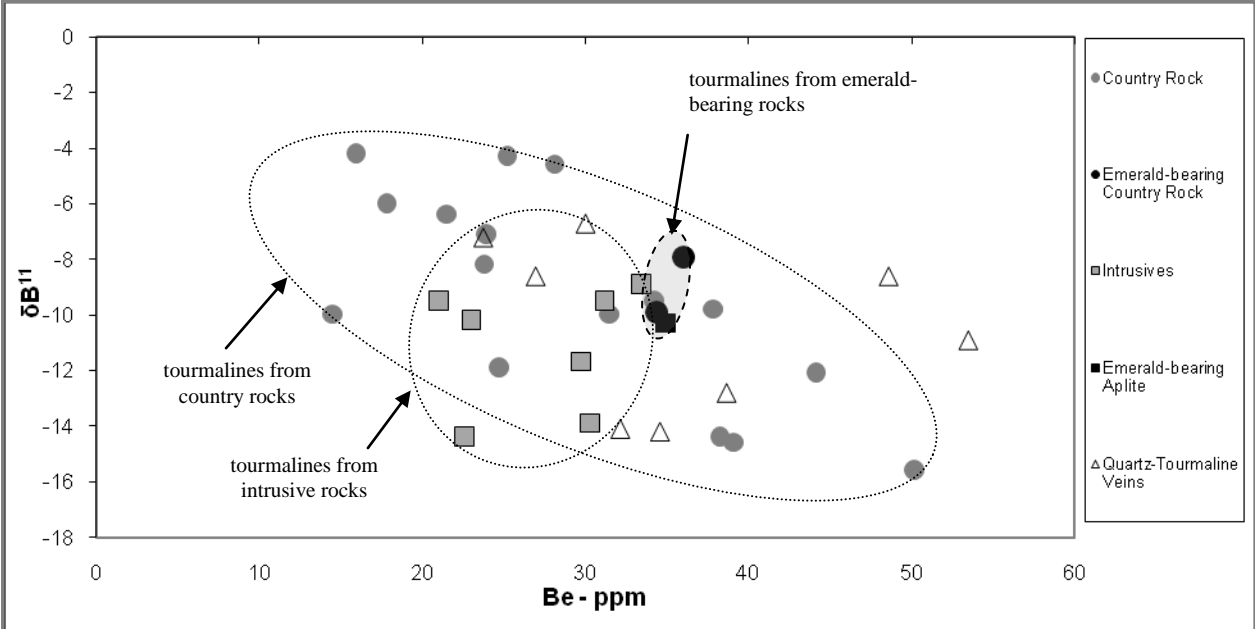


Figure 6B.

Table 1A. Average major-element compositions of Tsa da Glisza tourmalines (wt %).

Sample ¹	SiO ₂	TiO ₂	Al ₂ O ₃	Cr ₂ O ₃ ²	V ₂ O ₃ ²	B ₂ O ₃ ³	FeO	MgO	MnO	CaO	Na ₂ O	K ₂ O	H ₂ O ³	F	TOTAL
CR322807B	36.56	0.32	30.33	0.12	0.03	10.4	5.08	9.87	0.05	2.70	1.35	0.02	3.22	0.92	100.95
CR322915	35.09	0.16	31.03	0.00	0.00	10.4	5.92	8.81	0.02	2.24	1.55	0.01	3.22	0.76	99.23
CR322943	35.48	0.05	30.74	0.01	0.01	10.4	4.22	10.55	0.02	2.70	1.43	0.01	3.39	0.51	99.50
CR776T4	35.12	0.05	30.60	0.23	0.00	10.4	4.56	9.54	0.11	1.99	1.84	0.02	3.30	0.61	98.37
CRFW2	35.08	0.23	30.68	0.02	0.06	10.4	5.62	9.09	0.07	2.24	1.61	0.04	3.16	0.87	99.18
CRH0309B	35.12	0.32	31.58	0.05	0.05	10.4	6.33	7.87	0.00	1.74	1.67	0.02	3.59	0.02	98.74
CRH0425	35.70	0.31	30.74	0.40	0.02	10.4	5.54	9.25	0.00	1.69	1.94	0.01	3.51	0.25	99.76
CRH0432	35.23	0.55	31.59	0.00	0.05	10.4	5.78	8.64	0.01	1.95	1.76	0.01	3.49	0.29	99.74
CRHR3	35.22	0.33	32.24	0.02	0.02	10.4	5.04	8.66	0.03	1.53	1.81	0.02	3.59	0.06	98.97
CRHRT1	35.43	0.39	32.34	0.00	0.00	10.4	6.06	8.18	0.03	1.66	1.64	0.03	3.50	0.28	99.94
CRHRT6	36.17	0.31	30.54	0.32	0.05	10.4	4.43	9.78	0.02	2.23	1.53	0.02	3.40	0.48	99.68
CRMO3	35.38	0.21	32.51	0.14	0.00	10.4	5.35	8.52	0.07	1.60	1.78	0.03	3.33	0.65	99.97
CRMO5	36.43	0.13	33.64	0.06	0.02	10.4	3.23	8.96	0.03	1.32	1.93	0.01	3.69	0.00	99.85
CROZ5	35.48	0.06	30.20	0.08	0.01	10.4	4.61	10.27	0.01	2.62	1.45	0.01	3.36	0.51	99.08
CRT0640	35.62	0.27	31.05	0.07	0.01	10.4	4.59	9.88	0.02	1.99	1.83	0.01	3.41	0.46	99.62
CRT0643	35.78	0.50	32.00	0.11	0.00	10.4	5.68	7.55	0.01	1.37	1.96	0.02	3.62	0.00	99.01
mean CR	35.56	0.26	31.36	0.10	0.02	10.40	5.13	9.09	0.03	1.97	1.69	0.02	3.42	0.42	99.48
rel SD%	1.32	57.16	3.06	117.27	97.81	0.00	15.90	9.41	97.49	22.77	11.45	52.87	4.56	73.08	0.61
ECR322807	35.63	0.20	32.62	0.77	0.05	10.4	6.70	6.72	0.13	1.18	1.82	0.04	3.37	0.49	100.13
ECR322810	34.42	0.15	32.29	0.05	0.03	10.4	6.89	7.11	0.15	1.34	1.87	0.02	3.31	0.55	98.58
ECRFW5	36.02	0.13	31.17	1.98	0.06	10.4	5.76	7.65	0.08	1.65	1.70	0.03	3.37	0.52	100.53
mean ECR	35.36	0.16	32.03	0.94	0.05	10.40	6.45	7.16	0.12	1.39	1.80	0.03	3.35	0.52	99.75
rel SD%	2.36	23.63	2.38	104.39	31.56	0.00	9.38	6.51	28.59	17.43	4.80	26.81	1.03	6.46	1.03
GCO1	33.50	0.62	33.72	0.32	0.02	10.4	13.16	1.56	0.27	0.30	1.96	0.06	3.35	0.32	99.57
APT1	36.79	0.19	32.12	0.10	0.02	10.4	5.36	8.47	0.18	0.98	2.23	0.03	3.48	0.42	100.77
AH0429	33.72	0.79	32.93	0.00	0.00	10.4	12.88	2.09	0.56	0.33	2.33	0.06	3.32	0.44	99.84
AMO2	34.40	0.95	32.12	0.00	0.01	10.4	9.68	5.07	0.17	0.70	2.21	0.08	3.33	0.48	99.61
AMO6	35.96	0.39	33.09	0.13	0.00	10.4	6.24	7.14	0.15	0.81	2.32	0.03	3.29	0.75	100.72
ATC2	34.73	0.22	34.88	0.00	0.01	10.4	8.38	4.14	0.12	0.59	1.79	0.02	3.46	0.28	98.98
ATH1	34.81	0.26	31.56	0.09	0.05	10.4	5.45	8.86	0.03	2.18	1.62	0.02	3.48	0.26	99.07
EAPMT1	36.73	0.12	33.24	0.00	0.01	10.4	5.27	7.52	0.23	0.83	2.18	0.02	3.42	0.54	100.51
mean G-A	35.08	0.44	32.96	0.08	0.01	10.40	8.30	5.61	0.21	0.84	2.08	0.04	3.39	0.44	99.88
rel SD%	3.64	69.93	3.18	138.86	102.56	0.00	39.86	50.44	72.76	70.32	12.53	60.45	2.29	37.28	0.71
QT322807A	35.99	0.23	29.83	0.03	0.05	10.4	4.75	10.25	0.01	2.65	1.40	0.01	3.39	0.48	99.47
QTFW3	35.93	0.33	32.70	0.01	0.05	10.4	5.85	7.86	0.02	1.51	1.68	0.01	3.65	0.00	100.00
QTHRT3	35.62	0.31	32.07	0.02	0.01	10.4	6.55	7.76	0.09	1.41	1.70	0.01	3.58	0.09	99.63
QTM07 rim	34.88	0.70	32.77	0.00	0.00	10.4	11.21	3.41	0.22	0.38	2.13	0.05	3.40	0.36	99.91
QTM07 core	34.62	0.43	31.93	0.00	0.00	10.4	6.44	6.65	0.16	0.69	2.25	0.05	3.35	0.48	98.77
QTOZ2	35.51	0.31	30.54	0.13	0.00	10.4	5.45	9.46	0.04	2.03	1.67	0.02	3.52	0.19	99.28
QTOZ3	35.93	0.09	30.78	0.11	0.00	10.4	4.33	10.27	0.00	2.69	1.48	0.00	3.35	0.60	100.04
QTSUM1	35.01	0.55	31.42	0.00	0.02	10.4	6.99	7.92	0.00	1.50	1.73	0.01	3.58	0.03	99.16
QTT0642	35.95	0.17	33.93	0.00	0.00	10.4	4.43	8.19	0.02	1.13	2.00	0.01	3.67	0.01	99.89
mean QT	35.49	0.35	31.77	0.03	0.01	10.40	6.22	7.97	0.06	1.55	1.78	0.02	3.50	0.25	99.57
rel SD%	1.49	54.62	4.02	151.49	147.31	0.00	33.77	26.36	126.74	51.10	16.08	97.06	3.67	94.02	0.44

¹ prefix of sample identifies host lithology of tourmaline: "CR" - country rock; "ECR" - country rock containing emerald; "G" - granite; "A" - aplite; "EA" - aplite containing emerald; "QT" - quartz-tourmaline vein

² analyses by electron microprobe replaced by analyses by LA-ICP-MS

³ B₂O₃ as a fixed weight, and H₂O as the amount required to fill the F-site

Table 1B. Structural formulas of Tsa da Glisza tourmalines (atoms per formula unit - apfu)

Sample	X-SITE (apfu)				Y-SITE								Z-SITE			T-SITE			F-SITE				Cation Charge ¹⁰
	Na	Ca	K	Total X ¹	Fe	Mg ²	Mn	Al ²	Cr ³	V ³	Ti	Total Y ⁴	Al ⁵	Mg ⁵	Total Z ⁶	Si	Al ⁷	Total T ⁸	B	F	OH	Total F ⁹	
CR322807B	0.43	0.47	0.00	0.91	0.70	1.94	0.01	0.28	0.04	0.01	0.04	3.00	5.57	0.47	6.04	5.99	0.01	6.00	2.94	0.47	3.52	4.00	61.76
CR322915	0.50	0.40	0.00	0.90	0.83	1.79	0.00	0.35	0.00	0.01	0.02	3.00	5.62	0.40	6.02	5.86	0.14	6.00	3.00	0.40	3.59	3.99	61.80
CR322943	0.46	0.48	0.00	0.93	0.58	2.12	0.00	0.25	0.03	0.01	0.01	3.00	5.58	0.48	6.05	5.85	0.15	6.00	2.96	0.27	3.73	4.00	61.87
CR776T4	0.60	0.36	0.00	0.96	0.64	2.02	0.02	0.23	0.08	0.01	0.01	3.00	5.65	0.36	6.01	5.86	0.14	6.00	3.00	0.32	3.68	4.00	61.84
CRFW2	0.52	0.40	0.01	0.93	0.79	1.86	0.01	0.29	0.00	0.02	0.03	3.00	5.62	0.40	6.02	5.87	0.13	6.00	3.00	0.46	3.53	3.99	61.77
CRH0309B	0.54	0.31	0.00	0.85	0.88	1.64	0.00	0.38	0.03	0.02	0.04	3.00	5.64	0.31	5.95	5.84	0.16	6.00	2.98	0.01	3.98	3.99	62.00
CRH0425	0.62	0.30	0.00	0.92	0.76	1.98	0.00	0.15	0.06	0.01	0.04	3.00	5.73	0.30	6.02	5.89	0.11	6.00	2.96	0.13	3.87	4.00	61.94
CRH0432	0.56	0.34	0.00	0.91	0.80	1.78	0.00	0.32	0.03	0.00	0.07	3.00	5.64	0.34	5.99	5.82	0.18	6.00	2.96	0.15	3.85	4.00	61.92
CRHR3	0.58	0.27	0.00	0.86	0.70	1.86	0.00	0.39	0.00	0.01	0.04	3.00	5.71	0.27	5.99	5.82	0.18	6.00	2.97	0.03	3.96	3.99	61.98
CRHRT1	0.52	0.29	0.01	0.82	0.84	1.71	0.00	0.39	0.00	0.01	0.05	3.00	5.72	0.29	6.02	5.84	0.16	6.00	2.96	0.14	3.85	3.99	61.93
CRHRT6	0.49	0.39	0.00	0.89	0.61	2.01	0.00	0.31	0.01	0.01	0.04	3.00	5.60	0.39	5.99	5.97	0.03	6.00	2.96	0.25	3.75	4.00	61.88
CRMO3	0.57	0.28	0.01	0.86	0.74	1.81	0.01	0.36	0.05	0.01	0.03	3.00	5.77	0.28	6.05	5.82	0.18	6.00	2.96	0.34	3.66	4.00	61.83
CRMO5	0.61	0.23	0.00	0.84	0.44	1.94	0.00	0.59	0.02	0.01	0.02	3.00	5.74	0.23	5.97	5.90	0.10	6.00	2.91	0.00	3.99	3.99	62.00
CROZ5	0.47	0.47	0.00	0.93	0.64	2.08	0.00	0.27	0.00	0.00	0.01	3.00	5.55	0.47	6.02	5.90	0.10	6.00	2.99	0.27	3.73	4.00	61.86
CRT0640	0.58	0.35	0.00	0.94	0.63	2.08	0.00	0.23	0.01	0.01	0.03	3.00	5.68	0.35	6.04	5.88	0.12	6.00	2.96	0.24	3.76	4.00	61.88
CRT0643	0.63	0.24	0.00	0.88	0.79	1.62	0.00	0.52	0.00	0.01	0.06	3.00	5.64	0.24	5.88	5.92	0.08	6.00	2.97	0.00	4.00	4.00	62.00
mean CR	0.54	0.35	0.00	0.90	0.71	1.89	0.00	0.33	0.02	0.01	0.03	3.00	5.65	0.35	6.00	5.88	0.12	6.00	2.97	0.22	3.78	4.00	61.89
ECR322807	0.59	0.21	0.01	0.80	0.93	1.45	0.02	0.56	0.00	0.01	0.03	3.00	5.74	0.21	5.95	5.92	0.08	6.00	2.98	0.26	3.74	3.99	61.87
ECR322810	0.61	0.24	0.00	0.85	0.97	1.54	0.02	0.39	0.06	0.01	0.02	3.00	5.76	0.24	6.00	5.77	0.23	6.00	3.01	0.29	3.70	4.00	61.85
ECRFW5	0.55	0.29	0.01	0.85	0.80	1.59	0.01	0.38	0.19	0.01	0.02	3.00	5.65	0.29	5.94	5.95	0.05	6.00	2.97	0.27	3.72	3.99	61.86
mean ECR	0.58	0.25	0.01	0.83	0.90	1.53	0.02	0.44	0.09	0.01	0.02	3.00	5.72	0.25	5.96	5.88	0.12	6.00	2.99	0.27	3.72	3.99	61.86
GCO1	0.65	0.06	0.01	0.72	1.88	0.34	0.04	0.66	0.00	0.00	0.08	3.00	5.83	0.06	5.89	5.71	0.29	6.00	3.06	0.18	3.82	3.99	61.91
APT1	0.70	0.17	0.01	0.88	0.73	1.88	0.03	0.25	0.08	0.01	0.02	3.00	5.87	0.17	6.04	5.97	0.03	6.00	2.92	0.22	3.77	3.99	61.89
AH0429	0.77	0.06	0.01	0.84	1.83	0.47	0.08	0.47	0.05	0.01	0.10	3.00	5.84	0.06	5.90	5.72	0.28	6.00	3.05	0.24	3.76	4.00	61.88
AMO2	0.72	0.13	0.02	0.86	1.36	1.15	0.02	0.34	0.00	0.00	0.12	3.00	5.82	0.13	5.94	5.79	0.21	6.00	3.02	0.26	3.74	4.00	61.87
AMO6	0.74	0.14	0.01	0.89	0.86	1.61	0.02	0.46	0.00	0.00	0.05	3.00	5.85	0.14	6.00	5.91	0.09	6.00	2.95	0.39	3.61	4.00	61.80
ATC2	0.58	0.10	0.00	0.69	1.17	0.92	0.02	0.86	0.00	0.00	0.03	3.00	5.79	0.10	5.90	5.79	0.21	6.00	3.00	0.15	3.85	4.00	61.93
ATH1	0.52	0.39	0.00	0.91	0.76	1.81	0.00	0.37	0.02	0.01	0.03	3.00	5.60	0.39	5.98	5.79	0.21	6.00	2.98	0.13	3.86	4.00	61.93
EAPMT1	0.69	0.14	0.01	0.84	0.72	1.68	0.03	0.51	0.04	0.00	0.01	3.00	5.85	0.14	5.99	5.98	0.02	6.00	2.92	0.28	3.72	4.00	61.86
mean G-A	0.67	0.15	0.01	0.83	1.16	1.23	0.03	0.49	0.02	0.00	0.06	3.00	5.81	0.15	5.96	5.83	0.17	6.00	2.99	0.23	3.77	4.00	61.89
QT322807A	0.45	0.47	0.00	0.92	0.66	2.06	0.00	0.23	0.01	0.02	0.03	3.00	5.54	0.47	6.01	5.95	0.05	6.00	2.97	0.25	3.75	3.99	61.88
QTFW3	0.53	0.26	0.00	0.80	0.80	1.66	0.00	0.49	0.00	0.01	0.04	3.00	5.71	0.26	5.97	5.88	0.12	6.00	2.94	0.00	3.99	3.99	62.00
QTHRT3	0.54	0.25	0.00	0.80	0.90	1.66	0.01	0.36	0.02	0.01	0.04	3.00	5.76	0.25	6.00	5.88	0.12	6.00	2.96	0.05	3.94	3.99	61.98
QTM07 core	0.69	0.07	0.01	0.77	1.58	0.79	0.03	0.51	0.00	0.00	0.09	3.00	5.84	0.07	5.90	5.86	0.14	6.00	3.02	0.19	3.81	4.00	61.91
QTM07 rim	0.74	0.13	0.01	0.88	0.90	1.55	0.02	0.47	0.00	0.00	0.05	3.00	5.76	0.13	5.94	5.86	0.14	6.00	3.04	0.26	3.75	4.00	61.88
QTOZ2	0.54	0.36	0.00	0.90	0.76	1.98	0.01	0.18	0.03	0.01	0.04	3.00	5.66	0.36	6.02	5.88	0.12	6.00	2.97	0.10	3.89	3.99	61.95
QTOZ3	0.47	0.48	0.00	0.95	0.60	2.05	0.00	0.34	0.00	0.01	0.01	3.00	5.55	0.48	6.02	5.91	0.09	6.00	2.96	0.31	3.68	3.99	61.84
QTSUM1	0.56	0.27	0.00	0.83	0.97	1.70	0.00	0.25	0.00	0.01	0.07	3.00	5.73	0.27	6.00	5.82	0.18	6.00	2.99	0.02	3.98	3.99	61.99
QTT0642	0.63	0.20	0.00	0.83	0.60	1.79	0.00	0.57	0.00	0.01	0.02	3.00	5.78	0.20	5.98	5.85	0.15	6.00	2.92	0.00	3.99	3.99	62.00
mean QT	0.57	0.28	0.00	0.85	0.86	1.69	0.01	0.36	0.03	0.01	0.04	3.00	5.71	0.28	5.98	5.87	0.13	6.00	2.97	0.13	3.86	3.99	61.93

¹ Total X = Ca+Na+K, in atoms per formula unit

² Mg and Al that only occupy the Y-site

³ Cr and V arbitrarily assigned exclusively to the Y-site

⁴ Total Y = Fe+Mg+Mn+Al+Cr+V+Ti in that site, in atoms per formula unit

⁵ Mg and Al exclusively occupy the Z-site

⁶ Total Z = Al+Mg, in atoms per formula unit

⁷ the amount of Al required to fill the T-site

⁸ Total T = Si + Al, in atoms per formula unit

⁹ Total F = F+OH, in atoms per formula unit

¹⁰ Cation charge is equal to the sum of the charges of all cations, e.g. 0.5 Na = 0.5*1; 0.06 Ti = 0.06*4; etc.

Table 3. Boron isotope compositions of Tsa da Glisza tourmalines ($\delta^{11}\text{B}$).

Sample	$\delta^{11}\text{B}(\text{‰})^1$	range ²
CR322915	-9.5	
CR322943	-15.6	
CR322807B	-10.9	
CR776T4	-9.8	
CRFW2	-14.6	
CRH0309B	-4.6	
CRH0425	-10.0	
CRH0432	-8.2	
CRHR3	-11.9	
CRHRT1	-6.4	
CRHRT6	-7.1	
CRMO3	-4.2	
CRMO5	-6.0	
CROZ5	-12.1	
CRT0640	-4.3	
CRT0643	-14.4	
ECR322807	-9.9	
ECR322810	-7.9	-6 to -11
GCO1	-9.5	
APT1	-11.7	
AH0429	-9.5	
AMO2	-8.9	
AMO6	-10.2	
ATC2	-14.4	-11 to -17
ATH1	-13.9	
EAPMT1	-10.3	
QT322807A	-10.0	
QTFW3	-7.2	
QTHRT3	-8.6	
QTHR4	-11.1	
QTM07	-8.6	
QTOZ2	-12.8	
QTOZ3	-14.1	-12 to -16
QTSUM1	-14.2	
QTT0642	-6.7	

Analyses by SIMS; repeatability better than 1‰

¹ values are average of 2-3 points per sample

² range for samples with variation > 2‰

Table 4. Notable Pearson and Spearman correlation coefficients for Tsa da Glisza tourmalines.

Pair	Pearson	Spearman
Na-Ca	-0.883	-0.874
Fe-Mg ¹	-0.926	-0.817
Li-Zn	0.975	0.796
Ni-Co	0.746	0.747
Y-Yb	0.893	0.841
La-Ce	0.985	0.96
Cr-V	0.159	0.139

¹ total Mg, including Y-site and Z-site

Table 5. Summary of cluster analysis for Tsa da Glisza tourmalines.

	TOTAL	CR ¹	CR-E ²	GR ³	AP ⁴	AP-E ⁵	QTV ⁶
Cluster 1	23	15	0	0	1	0	7
Cluster 2	11	1	2	1	5	1	1
Cluster 1	23	15	0	0	1	0	7
Cluster 2	10	1	2	1	4	1	1
Cluster 3	1	0	0	0	1	0	0
Cluster 1	22	14	0	0	1	0	7
Cluster 2	9	1	2	1	3	1	1
Cluster 3	1	0	0	0	1	0	0
Cluster 4	2	1	0	0	1	0	0

¹ tourmalines from country rocks

² tourmalines from emerald-bearing country rocks

³ tourmalines from granite

⁴ tourmalines from aplites

⁵ tourmalines from emerald-bearing aplite

⁶ tourmalines from quartz-tourmaline veins

Table 6. Summary of discriminant function analysis.

MODEL 1 - NARROW COMPLETE				MODEL 2 - NARROW STEPWISE			
Classification matrix				Classification Matrix			
	E ¹	NE ²	%correct		E ¹	NE ²	%correct
E ¹	3	0	100	E ¹	3	0	100
NE ²	0	31	100	NE ²	3	28	90
Total	3	31	100	Total	6	28	91
Jackknifed classification matrix				Jackknifed classification matrix			
	E ¹	NE ²	%correct		E ¹	NE ²	%correct
E ¹	2	1	67	E ¹	3	0	100
NE ²	12	19	61	NE ²	4	27	87
Total	14	20	62	Total	7	27	88
MODEL 3 - WIDE COMPLETE				MODEL 4 - WIDE STEPWISE			
Classification matrix				Classification matrix			
	E ³	NE ⁴	%correct		E ³	NE ⁴	%correct
E ³	11	0	100	E ³	10	1	91
NE ⁴	1	22	96	NE ⁴	3	20	87
Total	12	22	97	Total	13	21	88
Jackknifed classification matrix				Jackknifed classification matrix			
	E ³	NE ⁴	%correct		E ³	NE ⁴	%correct
E ³	4	7	36	E ³	9	2	82
NE ⁴	10	13	57	NE ⁴	5	18	78
Total	14	20	50	Total	14	20	79

¹ tourmalines from rocks with emerald in sample

² tourmalines from rocks without emeralds in sample

³ tourmalines from rocks near emerald mineralization, within approximately 10 meters

⁴ tourmalines from rocks with no known nearby emerald mineralization